

Non-Abelian gauge theories of Fermi systems: Quantum-chromodynamic theory of highly condensed matter

Varouzhan Baluni

Center for Theoretical Physics, Laboratory for Nuclear Science and Department of Physics, Massachusetts Institute of Technology, Cambridge, Massachusetts 02139

(Received 3 October 1977)

A systematic perturbation theory for high-density quark gas is developed. The ground-state thermodynamic potential is evaluated up to the second order in the Gell-Mann-Low coupling $\alpha_s(M)$. Phenomenological analysis of the resulting equation of state suggests that the neutron-quark matter phase transition occurs at neutron matter densities $n_B < 2$ baryon/fm³ provided $0.2 < \alpha_s(3 \text{ GeV}) < 0.3$. The result supports the conjecture that superheavy stellar objects may exist in the quark rather than in the neutron phase. The production of quark matter in heavy-ion collisions is also discussed briefly.

I. INTRODUCTION

This paper is a detailed and extensive account of recently reported results on the quantum-chromodynamic theory of highly condensed matter, i.e., quantum theory of colored quark gas.¹

Quantum chromodynamics (QCD) is believed to be the underlying theory of hadrons. Its fundamental entities are quarks (fermions) and gluons (vector bosons) interlocked by the non-Abelian local gauge symmetry. Owing to its remarkable property of asymptotic freedom, QCD is believed to provide a theoretical foundation for naive parton models; the latter appear to be a lowest-order approximation to perturbative aspects of QCD.

It is frustrating that until now the experimental successes of parton models served as the only *raison d'être* for QCD. Quantitative tests of QCD are still lacking both for experimental and theoretical reasons.

At present, perturbative methods are known to be the only available tools for a theoretical analysis. Unfortunately, physical quantities amenable to such analysis are extremely limited. Well-known examples of these quantities are the electron-positron annihilation cross section and moments of structure functions of deep-inelastic lepton production.^{2,3} Two more candidates which have been recently proposed are the thermodynamic quantities of the quark gas¹ and the jet production characteristics in the electron-positron annihilation.⁴ It is difficult to overestimate the physical significance of these unique quantities which may determine the predictive power and limitations of perturbative aspects of QCD.

Applicability of perturbation theory is known to be hampered by infrared divergences and mass singularities. The former are generated by the

masslessness of gluons, whereas the latter stem from the small mass of some quarks. For very different reasons the above-mentioned quantities are devoid of infrared divergences and mass singularities.

In the case of the electron-positron cross section this property is ensured by the Kinoshita theorem.^{5,6} The moments of the deep-inelastic structure functions are amenable to perturbative treatment since they are given by the coefficient functions in the Wilson operator-product expansion of two currents. The Wilson expansion disentangles the finite short-distance effects in the product of two currents absorbing them in the coefficient functions.⁷ Thermodynamic quantities of the zero-temperature quark gas have well-defined perturbative expansions due to Pauli's exclusion principle as first pointed out in Ref. 1. The validity of the perturbative analysis of jets has been conjectured and verified explicitly to the lowest nontrivial order in the interaction coupling.⁴

It was pointed out many years ago that infrared divergences and mass singularities are due to the degeneracy of physical states with massless particles.⁶ States differing by a number of soft particles are almost degenerate and in general make nondegenerate perturbation theory inapplicable. Obviously, the above argument does not hold when transitions between these states are forbidden. The ground state of the massless quark gas is one of these remarkable exceptions. The Pauli exclusion principle, activated by the existence of the Fermi sea, prohibits quarks inside the Fermi sea to absorb soft gluons and thereby prevents infrared divergences. Quarks on the top of the Fermi sea occupy a vanishing phase-space volume and, hence, do not contribute to thermodynamic quantities. Furthermore, the addition of soft quark-antiquark pairs to the Fermi sea is

forbidden and, therefore, mass singularities are also prevented.

One suspects that thermodynamic quantities of massless quark gas at *nonzero* temperatures are also well defined in the perturbation theory. However, we are not aware of a simple argument proving this conjecture.

Interest in the quark gas was originally motivated by an interesting suggestion that in the dense stellar objects, matter exists in the quark rather than in the neutron phase.^{8,9} The suggestion spurred a series of papers on the feasibility of a neutron-quark-matter phase transition. The studies have been carried out in the framework of the MIT bag model^{10-13a} and the Born approximation of QCD.^{13b-15} The former contains the bag constant to account for confining forces and assumes a constant strength of interactions, whereas the latter uses a density-dependent effective charge defined according to the Gell-Mann-Low equation. Evidently, the ultimate theory of phase transitions should incorporate the complementary aspects of both approaches in a consistent fashion.

Calculations of the thermodynamic quantities beyond the Born approximation have been carried out by two different methods.^{1,16} The approach of Ref. 1 will be presented in detail in the subsequent sections. To facilitate the readers' orientation we comment on Refs. 16 in the conclusion of this paper.

This paper is organized as follows: In Sec. II the formalism for the temperature Green's functions is reviewed with an emphasis on the regularization and subtraction schemes. The nonzero-temperature formalism is employed to regulate singularities stemming from the discontinuous character of the zero-temperature Fermi distribution. In Secs. II and III, the zero-temperature thermodynamic potential of the quark gas is expressed in terms of *bona fide* Feynman diagrams. This reduction is carried out to the fourth order of the interaction coupling with a careful zero-temperature limiting procedure. Infrared and mass singularities arising at this stage are controlled by the dimensional regularization. Section IV contains explicit calculations of the fourth-order thermodynamic potential; in Sec. V the equation of state of the quark gas is analyzed and neutron-quark-matter phase transition is discussed; in Sec. VI the results are summarized, and their implications for neutron stars and heavy-ion collisions are briefly discussed. Finally, the second-order expressions for unrenormalized propagators and the quark-gluon vertex in the general covariant gauge are supplied in the Appendix.

II. FORMALISM FOR THE TEMPERATURE GREEN'S FUNCTIONS

In this section the formal apparatus of the *temperature* Green's functions will be concisely reviewed. The derivation will be based on the functional integral representation of the thermo-dynamic potential Ω . Since the system under consideration has a non-Abelian gauge symmetry, its quantization requires special attention. This problem will be discussed first and the appropriate Feynman rules will be hence defined. Next, the renormalization scheme and subtraction prescription will be described based on the Dyson-Schwinger equations.

A. Thermodynamic potential

Let $\hat{H}(\hat{p}, \hat{q})$ be the Hamiltonian of the system with canonically conjugate variables \hat{p}, \hat{q} and conserved quantities $\hat{O}_A(\hat{p}, \hat{q}), A=1, \dots, K$. The thermodynamic potential of the system Ω is defined in terms of the partition function Z by

$$Z = \text{Tr} \exp \left[-\beta \left(\hat{H} - \sum_A \mu_A \hat{O}_A \right) \right], \quad (2.1a)$$

$$\Omega = -\frac{1}{\beta} \ln Z, \quad (2.1b)$$

where β is the inverse temperature and the μ_A 's are chemical potentials appearing as Lagrange multipliers, and being fixed by eigenvalues of the O_A 's. The expression (2.1a) for Z represents the trace of the Euclidean evolution operator $\exp(-i\hat{H}_{\text{eff}})_{t=-i\beta}$ of the system with the Hamiltonian $\hat{H}_{\text{eff}} = \hat{H} - \sum \mu_A \hat{O}_A$. More specifically it is a direct sum of Euclidean transition amplitudes between *identical* states.

Therefore, Eq. (2.1a) can be recast in the functional form. Namely, by the standard method, it can be reduced to a path integral along classical trajectories. However, special care should be exercised defining the phase space $\{p(t), q(t)\}$ of classical trajectories since the classical system of interest obeys first-class constraints. An elegant definition of this phase space is given by Faddeev^{17a} in the quantum field theory of constrained classical systems ($t=\infty$). The method directly applies to Eq. (2.1) provided that the class of classical trajectories considered is restricted to periodic (antiperiodic) paths $q(0) = \pm q(-i\beta)$ in the case of bosonic (fermionic) degrees since only *diagonal* matrix elements $\langle q | \exp(-\beta H_{\text{eff}}) | q \rangle$ appear in Eq. (2.1). The distinct choice of periodicity conditions ensures a correct spin-statistics relation; namely it implies the Bose-Einstein and Fermi-Dirac distributions for free Bose and Fermi systems, respectively (see Sec. IIIA). Thus, one derives the functional representation for the partition function of the Fermi system with non-Abelian gauge interactions^{18,19}:

$$Z\{\eta, J\} = N(\beta) \int \mathcal{D}\psi \mathcal{D}\bar{\psi} \mathcal{D}C \mathcal{D}C^* \mathcal{D}A_\mu \exp \left\{ \int_0^\beta d\tau \int d^3x \left[\mathcal{L}_{\text{eff}}(x) + J^\mu(x) A_\mu(x) + \bar{\psi}(x) \eta(x) + \bar{\eta}(x) \psi(x) \right] \right\}, \quad (2.2)$$

where the normalization constant $N(\beta)$ is irrelevant for the subsequent discussion. In Eq. (2.2) anticommuting fermionic $[\eta(x)]$ and commuting gluonic $[J_\mu(x)]$ external sources are incorporated for later purposes. The quark and gluon degrees are represented by anticommuting fields $\psi(x) = \{\psi^{\alpha,a,i}(x)\}$ and commuting fields $A_\mu(x) = \{A_\mu^i(x)\}$ with superscripts (α, a, i) designating the Dirac (α) , flavor (a) , and color (i) indices, respectively. They will be suppressed whenever it does not cause confusion. The anticommuting fields $C(x) = \{C^i(x)\}$ are the Faddeev-Popov^{17b} ghosts which are artifacts of previously mentioned first-class constraints. The effective Lagrangian \mathcal{L}_{eff} is given by²⁰

$$\mathcal{L}_{\text{eff}}(x) = \mathcal{L}_0(x) + \mathcal{L}_{\text{int}}(x), \quad (2.3a)$$

$$\mathcal{L}_0(x) = \bar{\psi}(i\vec{\partial} - m_0)\psi + \frac{1}{2} A^\nu \left[g_{\mu\nu} \partial^2 - \left(1 - \frac{1}{\alpha_0}\right) \partial_\mu \partial_\nu \right] A^\nu - C^* \partial^2 C, \quad (2.3b)$$

$$\mathcal{L}_{\text{int}}(x) = -g_0 \bar{\psi} \gamma^\mu A_\mu^i \lambda^i \psi + i g_0 (A_\mu T^i A_\nu) \partial^\mu A^\nu + \frac{1}{4} g_0^2 (A_\mu T^i A_\nu) (A^\mu T^i A^\nu) + i g_0 (\partial_\mu C^* T^i C) A_\mu^i, \quad (2.3c)$$

with $\vec{\partial} = \not{\partial} + \mu \gamma_4$, $\mu = \mu_A \cdot O^A$, where the diagonal matrices O^A define conserved fermionic charges $\hat{O}^A(x) = \bar{\psi}(x) i \gamma_4 O^A \psi(x)$, e.g., baryon number ($A=B$), electric charge ($A=Q$), strangeness ($A=S$), etc. In Eq. (2.3b) the α_0 is a gauge-fixing parameter.

From Eqs. (2.2) and (2.3) one immediately infers the Feynman rules. They are summarized in Fig. 1. Observe that as a result of the (anti) periodicity condition, the time components of the momenta are discrete, namely, the gluon momenta $K = (\vec{K}, K^4 = 2\pi m\beta)$, whereas the quark and ghost momenta $p = (\vec{p}, p^4 = 2\pi(m + \frac{1}{2})\beta)$ m being an arbitrary integer. Therefore, each loop contains an integration over spatial components as well as a summation over the "time" components of the internal momenta p , i.e.,

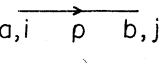
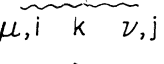
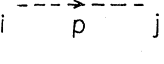

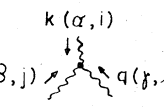
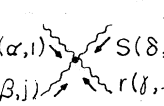
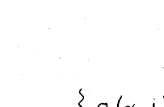
(a)		$S_{ai, bj}(p) = -(\not{p} - m)^{-1} \delta_{ab} \delta_{ij}$
(b)		$\mathcal{D}_{\mu i, \nu j}(k) = \frac{1}{k^2} \left[g_{\mu\nu} - (1 - \alpha) \frac{k_\mu k_\nu}{k^2} \right] \delta_{ij}$
(c)		$G_{ij}(p) = -\frac{1}{p^2} \delta_{ij}$
(d)		$\Gamma^{(0)} = -g \lambda^i \gamma^\mu$
(e)		$M_2^{(0)} = -ig C_{ijl} [g_{\alpha\gamma} (r-q)_\beta + g_{\alpha\beta} (k-r)_\gamma + g_{\gamma\beta} (q-k)_\alpha]$
(f)		$M_3^{(0)} = -g^2 [C_{imn} C_{nj} (g_{\alpha\beta} g_{\delta\gamma} - g_{\alpha\gamma} g_{\delta\beta}) + C_{ijn} C_{nm\ell} (g_{\alpha\delta} g_{\beta\gamma} - g_{\alpha\beta} g_{\delta\gamma}) + C_{i\ell n} C_{nmj} (g_{\alpha\delta} g_{\beta\gamma} - g_{\alpha\gamma} g_{\delta\beta})]$
(g)		$\Upsilon^{(0)} = -ig C_{ij\ell} k_\alpha$

FIG. 1. Euclidean Feynman rules: (a) quark propagator with $\vec{p} = \vec{p} + i\gamma_n \mu$, (b) gluon propagator, (c) ghost propagator, (d) quark-gluon vertex, (e) three-gluon vertex, (f) four-gluon vertex, (g) ghost-ghost vertex. The quark and ghost momenta are $p = (\vec{p}, p^4 = (2\pi/\beta)(m + \frac{1}{2}))$ and the gluon momenta are $q = (\vec{q}, q^4 = (2\pi/\beta)m)$, where m is an integer.

$$\frac{1}{\beta} \sum_m \frac{1}{(2\pi)^3} \int d\vec{p} \dots$$

Now the renormalization of the theory will be explained heuristically. Observe that at zero temperature ($1/\beta=0$) and at zero fermion density ($\mu_A=0$) Eq. (2.2) reduces to the Euclidean generating functional of QCD. Furthermore, the temperature and density effects apparently do not affect the ultraviolet behavior of QCD. In other words, the renormalization scheme of QCD should be adequate to render Eq. (2.2) finite in all orders of perturbation theory. We will proceed with this assumption in mind.

Ultraviolet divergences will be regulated via analytical continuation of the space dimension from 3 to $n-1$.²¹ The dimensional regularization exhibits ultraviolet as well as infrared divergences in the form of poles at $n=4$. The important virtue of the above approach is that it automatic-

ally regulates all infrared singularities which, as explained in the Introduction, occur in all intermediate steps of our calculations.

The renormalization procedure is known to be a special rearrangement of the perturbation series which allows the absorption of all ultraviolet singularities (poles) into the renormalized parameters of the theory. The renormalization is formally achieved by rescaling of fields, sources, and parameters g_0, α_0, m_0 , and μ_A as follows:

$$\psi = Z_2^{1/2} \psi_R, \quad A_\mu = Z_3^{1/2} A_\mu^R, \quad C = Z_{3g}^{1/2} C_R, \quad (2.4a)$$

$$\eta = Z_2^{-1/2} \eta_R, \quad J_\mu = Z_3^{-1/2} J_\mu^R, \quad (2.4b)$$

$$g_0 = Z_1 Z_2^{-1} Z_3^{-1/2} g_R, \quad (2.4c)$$

$$m_0 = Z_m Z_2^{-1} m_R, \quad \mu_A = Z_A Z_2^{-1} \mu_A^R, \quad \alpha_0 = Z_3 \alpha_R, \quad (2.4d)$$

which leads to the renormalized partition function

$$Z\{\eta_R, J_R\} = N(\beta) \int \mathcal{D}\psi_R \mathcal{D}\bar{\psi}_R \mathcal{D}C_R \mathcal{D}C_R^* \mathcal{D}A_\mu^R \exp \left\{ \int d^n x [\mathcal{L}_0^R(x) + \mathcal{L}_{\text{int}}^R(x) + J_\mu^R(x) A_\mu^R(x) + \bar{\psi}_R(x) \eta_R(x) + \bar{\eta}_R(x) \psi_R(x)] \right\}, \quad (2.5)$$

where

$$\int d^n x (\dots) \equiv \int_0^\beta d\tau \int d^{n-1} x (\dots), \quad (2.6a)$$

$$\mathcal{L}_0^R(x) = \bar{\psi}_R (Z_2 i \not{\partial} + Z_A \mu_A^R i \gamma_n O^A - Z_m m_R) \psi_R + \frac{1}{2} A_\mu^R \left[Z_3 (g_{\mu\nu} \partial^2 - \partial_\mu \partial_\nu) + \frac{1}{\alpha_R} \partial_\mu \partial_\nu \right] A_\nu^R - Z_{3g} C_R^* \partial^2 C_R, \quad (2.6b)$$

$$\mathcal{L}_{\text{int}}^R(x) = -Z_{1gR} \bar{\psi}_R \gamma^\mu A_\mu^R i \lambda^i \psi_R + i Z_{1V} g_R (A_\mu^R T^i A_\nu^R) \partial^\mu A_\nu^R + \frac{1}{4} Z_{1V} g_R^2 (A_\mu^R T^i A_\nu^R) (A_\mu^R T^i A_\nu^R) + i Z_{1g} g_R (\partial_\mu C_R^* T^i C_R) A_{Ri}^\mu. \quad (2.6c)$$

Henceforth, the index R designating the renormalized quantities ψ_R, g_R , etc. will be omitted. All of the renormalization constants exhibited above are not linearly independent because of the Ward-Slavnov gauge identities. It will be convenient to choose $\{Z_{1,2}, Z_{3V}, Z_{3g}\}$ as a set of linearly independent renormalization constants. It will not be necessary to specify the relation of the remaining constants Z_{1V}, \bar{Z}_{1V} , and Z_{1g} to the above set, since the corresponding vertices AAA , $AAAA$, and CCA will not be encountered subsequently. The Z_A 's can be chosen to be equal to Z_2 due to the Abelian gauge identities (see below).

The renormalization constants $\{Z_i\}$ are given by a double series in the renormalized coupling g and inverse powers of $(n-4)$ (Ref. 22)

$$Z_i = \sum_{m,k=0}^{\infty} a_{mk}(i) g^m (n-4)^{-k}. \quad (2.7)$$

There exists an arbitrariness in the choice of coefficients of regular terms $\{a_{mk}(i), k=0\}$. Their

specification fixes the theory completely in terms of the parameters g, μ_A , and m which is accomplished by various subtraction schemes discussed in detail in the following subsections.

In conclusion, we define the renormalized fermion and gluon propagators in terms of functional derivatives of the generating functional $W\{\eta, J\} = \ln Z\{\eta, J\}$ [cf. Eqs. (2.1) and (2.5)].

$$S'(x, y) = - \frac{\delta^2 W\{\eta, J\}}{\delta \bar{\eta}(x) \delta \eta(y)} \Big|_{\eta=J=0}, \quad (2.8a)$$

$$\mathcal{D}'_{\mu\nu}(x, y) = \frac{\delta^2 W\{\eta, J\}}{\delta A_\mu(x) \delta A_\nu(y)} \Big|_{\eta=J=0}. \quad (2.8b)$$

Observe that the normalization coefficient $N(\beta)$ of Eq. (2.5) cancels in the above definitions.

B. Renormalized fermion propagator

The propagator (2.8a) obeys the Dyson equation implied by the invariance of the partition function (2.5) under translations of fermion fields $\bar{\psi}$ and ψ :

$$\bar{\psi}(x) \rightarrow \bar{\psi}'(x) = \bar{\psi}(x) + \bar{\alpha}(x), \quad (2.9a)$$

$$\psi(x) \rightarrow \psi'(x) = \psi(x) + \alpha(x), \quad (2.9b)$$

where $\bar{\alpha}$ and α are anticommuting elements. We perform the transformation (2.9a) in Eq. (2.5). Noting the invariance of the integration measure $\mathcal{D}\psi$ and the requirement that the coefficient of $\bar{\alpha}(x)$ must vanish, one obtains

$$(Z_2 i \not{\partial}_x + Z_A i \gamma_n O^A \mu_A - Z_m m) \langle \psi(x) \rangle + (-Z_1 \gamma^\mu \lambda^i g) \langle \psi(x) A_\mu^i(x) \rangle + \eta(x) \langle 1 \rangle = 0. \quad (2.10)$$

Here the following notation has been used

$$\begin{aligned} \langle \dots \rangle = N(\beta) \int \mathcal{D}\psi \mathcal{D}\bar{\psi} \mathcal{D}C \mathcal{D}C^* \mathcal{D}A_\mu \langle \dots \rangle \\ \times \exp \left\{ \int d^n x [\mathcal{L}(x) + J_\mu(x) A^\mu(x) \right. \\ \left. + \bar{\psi}(x) \eta(x) + \bar{\eta}(x) \psi(x)] \right\}. \end{aligned} \quad (2.11)$$

Acting on Eq. (2.10) by $\delta/\delta\eta(y)$ and recalling Eqs. (2.8), one immediately derives the Dyson equation for the fermion propagator

$$(Z_2 i \not{\partial}_x + Z_A i \gamma_n O^A \mu_A - Z_m m) S'(x, y) + \int d^n \xi \Sigma(x, \xi) S'(\xi, y) = -\delta^n(x - y), \quad (2.12)$$

where the unrenormalized fermion self-energy operator Σ has been introduced via the relation

$$\begin{aligned} (-Z_1 g \gamma^\mu \lambda^i) \frac{\langle \psi(x) A_\mu^i(z) \bar{\psi}(y) \rangle}{\langle 1 \rangle} \Big|_{\eta=J=0} \\ \equiv \int \Sigma(x, \xi) S'(\xi, y) d^n \xi. \end{aligned} \quad (2.13)$$

Notice that Σ is diagonal in flavor and color indices. It is easy to express Σ in terms of the $\psi\bar{\psi}A$ proper vertex function Γ . The latter is defined by

$$\begin{aligned} \frac{\langle \psi(x) A_\mu^i(z) \bar{\psi}(y) \rangle}{\langle 1 \rangle} \Big|_{\eta=J=0} = \int S'(x, \xi) \Gamma_\nu^i(\xi, \eta | \xi) \\ \times S'(\eta, y) \mathcal{D}_{\nu\mu}^{ij}(\xi, z) d^n \xi d^n \eta d^n z \end{aligned} \quad (2.14)$$

which, being compared with Eq. (2.13), leads to the desired equation

$$\begin{aligned} \Sigma(x, y) = (-Z_1 g \gamma^\mu \lambda^i) \int S'(x, \xi) \Gamma_\nu^i(\xi, y) \\ \times \mathcal{D}_{\mu, ij}^{\nu}(\xi, x) d^n \xi d^n z. \end{aligned} \quad (2.15)$$

Using translational invariance properties of the above functions $S'(x, y) \equiv S'(x - y)$ etc. and per-

forming the Fourier transformation, Eq. (2.12) may be rewritten concisely as

$$[Z_2 \not{p} + i Z_A \gamma_n O_A \mu_A - Z_m m + \Sigma(p)] S'(p) = -1, \quad (2.16)$$

where

$$S'(p) = \int d^n x e^{ipx} S'(x), \quad (2.17a)$$

$$\Sigma(p) = \int d^n x e^{ipx} \Sigma(x). \quad (2.17b)$$

Notice that the formal functional structure of the above equations is analogous to those of ordinary QCD except for the integration measure (2.6a) and the presence of terms with $\mu_A \neq 0$.

We turn to the subtraction scheme to fix the renormalization constants $Z_{1,2}$, Z_m , and $\{Z_A\}$. Consider the zero-temperature ($1/\beta=0$) and zero-density limit ($\mu_A=0$) of Eq. (2.16). Designating quantities in this limit as $S'_0(p)$, $\Sigma_0(p)$, etc., one obtains

$$[Z_2 \not{p} - Z_m m + \Sigma_0(p)] S'_0(p) = -1, \quad (2.18)$$

where the "time" component of the n -vector p_μ is a continuous rather than a discrete variable. Let us perform the standard decomposition

$$\Sigma_0(p) = \not{p} \Sigma_1(p^2) + m \Sigma_2(p^2). \quad (2.19)$$

Now we are in a position to carry out the subtractions and to define the renormalized self-energy operator as

$$\Sigma_{0R}(p) = \not{p} \Sigma_{1R}(p^2) + m \Sigma_{2R}(p^2), \quad (2.20)$$

with

$$\Sigma_{1R}(p^2) = \Sigma_1(p^2) - \Sigma_1(-M^2), \quad (2.21a)$$

$$\Sigma_{2R}(p^2) = \Sigma_2(p^2) - \Sigma_2(m^2) - \Sigma_1(m^2) + \Sigma_1(-M^2), \quad (2.21b)$$

the $p^2 = -M^2$ being an arbitrary Euclidean point. Then Eq. (2.18) may be recast in the form

$$[\not{p} - m + \Sigma_{0R}(p)] S'_0(p) = -1 \quad (2.22)$$

provided that Z_2 and Z_m are chosen to be

$$Z_2 = 1 - \Sigma_1(-M^2), \quad (2.23a)$$

$$Z_m = 1 - \Sigma_1(-M^2) + \Sigma_1(m^2) + \Sigma_2(m^2). \quad (2.23b)$$

It is important to emphasize that the subtraction scheme (2.21) and (2.23) ensures that the zero in $S'_0(p)$ is at $\not{p} = m$ and does not generate infrared divergences due to the fact that in perturbation theory $\Sigma_{1,2}(p^2)$ have only logarithmic ultraviolet divergences. In passing note that $\Sigma_{1,2}(p^2)$ are analytic in the complex p^2 plane with a cut along the real semiaxis (m^2, ∞) .

Finally, let us prove that $Z_A = Z_2$. The relevant renormalized vertex Γ_μ^A is defined by [cf. Eq. (2.14)]

$$\langle \psi(z) [\psi(x) O^A i\gamma_\mu \psi(x)] \bar{\psi}(y) \rangle / \langle 1 \rangle \Big|_{\eta=J=0} \\ \equiv Z_A \int d^n \xi d^n \eta S'(z, \xi) \Gamma_\mu^A(\xi, \eta | x) S(\eta, y). \quad (2.24)$$

The Γ_μ^A obey the Abelian gauge identity. Indeed one can derive the identity conjugate to Eq. (2.10):

$$\langle \bar{\psi}(x) \rangle (-Z_2 i \not{\partial}_x + Z_A i \gamma_n O^A \mu_A - Z_m m) \\ + \langle \bar{\psi}(x) A_\mu^i(x) \rangle (-Z_1 \gamma^\mu \lambda^i g) + \bar{\eta}(x) \langle 1 \rangle = 0. \quad (2.25)$$

Operating on Eqs. (2.10) and (2.25) by

$$\left(\frac{\delta}{\delta \eta(x)} O^A \right) \frac{\delta}{\delta \bar{\eta}(z)} \frac{\delta}{\delta \eta(y)}$$

and

$$\left(O^A \frac{\delta}{\delta \bar{\eta}(x)} \right) \frac{\delta}{\delta \bar{\eta}(z)} \frac{\delta}{\delta \eta(y)},$$

respectively, and subtracting the resulting expressions, one obtains

$$Z_2 \partial_x^\mu \langle \psi(z) [\bar{\psi}(x) O^A i\gamma_\mu \psi(x)] \bar{\psi}(y) \rangle \\ + \delta^n(x-y) \langle \psi(z) \bar{\psi}(x) \rangle O^A - \delta^n(x-z) O^A \langle \psi(x) \bar{\psi}(y) \rangle = 0. \quad (2.26)$$

Combining Eqs. (2.8a), (2.24), and (2.26) we arrive at the identity

$$(Z_2/Z_A) \partial_x^\mu \Gamma_\mu^A(z, y | x) = -\delta^n(z-x) O^A S'^{-1}(x, y) \\ + \delta^n(y-x) S'^{-1}(z, x) O^A. \quad (2.27)$$

In the limit $1/\beta = 0$ and $\mu_A = 0$ the Fourier transform of Eq. (2.27) reduces to

$$(Z_2/Z_A) (-iq^\mu) \Gamma_{0\mu}^A(p, p+q | q) \\ = -O^A [S_0'^{-1}(p+q) - S_0'^{-1}(p)], \quad (2.28)$$

where

$$\Gamma_{0\mu}^A(p_1, p_2 | q) \delta^n(p_1 - p_2 - q) \\ = \int d^n z d^n y d^n x e^{i(p_1 x - p_2 y + q x)} \Gamma_{0\mu}^A(z, y | x).$$

Furthermore, by the use of Eqs. (2.19)–(2.22) and the decomposition

$$\Gamma_{0\mu}^A(p, p | 0) = iO^A [\gamma_\mu \Gamma_1^A(p^2) + p_\mu \not{\partial} \Gamma_2^A(p^2) + p_\mu \Gamma_3^A(p^2)] \quad (2.29)$$

Eq. (2.28) leads to the desired relation

$$Z_A = Z_2, \quad (2.30a)$$

provided the subtraction prescription for the primitively divergent term Γ_1^A is fixed by

$$\Gamma_1^A(-M^2) = 1. \quad (2.30b)$$

A similar subtraction convention may be adopted for the renormalized $\bar{\psi}\psi A$ vertex

$$\Gamma_{0\mu}^i(p, p | 0) = -g\lambda^i [\gamma_\mu \Gamma_{1R}(p^2) + p_\mu \not{\partial} \Gamma_{2R}(p^2) \\ + p_\mu \Gamma_{3R}(p^2)], \quad (2.31a)$$

$$\Gamma_{1R}(-M^2) = 1. \quad (2.31b)$$

Since $\Gamma_{1R}(p^2)$ is related to its unrenormalized counterpart $\Gamma_1(p^2)$ by $\Gamma_{1R} = Z_1 \Gamma_1$, Eq. (2.31b) implies

$$Z_1^{-1} = \Gamma_1(-M^2). \quad (2.32)$$

Returning to Eq. (16) one may summarize the preceding analysis in the form

$$[S^{-1}(p) - \Sigma_R(p)] S'(p) = 1, \quad (2.33)$$

with

$$\Sigma_R(p) = \Sigma(p) - (Z_2 - 1) S^{-1}(p) - m(Z_m - Z_2), \quad (2.34a)$$

$$\Sigma(p) = (-Z_1 g \gamma_\mu \lambda^i) \frac{1}{\beta} \sum_m \frac{d^{n-1} q}{(2\pi)^{n-1}} S'(p-q) \\ \times \Gamma_\nu^i(p-q, p | q) \mathfrak{D}'_{ij}{}^{\nu\mu}(q), \quad (2.34b)$$

$$q = \left\{ q^n = \frac{2\pi}{\beta} m, \vec{q} \right\}.$$

Here Z_2 , Z_m , and Z_1 are determined by Eqs. (2.23a), (2.23b), and (2.32), respectively.

It is important to indicate the M dependence of the renormalized coupling $g(M)$ and renormalized mass $m(M)$ implied by Eqs. (2.4). Also notice from Eqs. (2.4d), (2.30a) that the renormalized chemical potential coincides with its bare counterpart and thereby is independent of M .

Obviously $Z_{1,2}$ and Z_m become diagonal matrices different from the unit matrix when the flavor symmetry is broken by the mass term $\bar{\psi} m_0 \psi$. This point will be implicit throughout the subsequent discussion.

C. Renormalized gluon propagator

The gluon propagator (2.8b) obeys the Dyson equation implied by the invariance of the partition function (2.5) under translations of gluon fields $A_\mu(x) \rightarrow A'_\mu(x) = A_\mu(x) + a_\mu(x)$. Owing to the invariance of the integration measure $\mathfrak{D}A'_\mu = \mathfrak{D}A_\mu$ the coefficient of the infinitesimal element $a_\mu(x)$ yields [cf. Eq. (2.12)]

$$[Z_3 (g_{\mu\rho} \partial^2 - \partial_\mu \partial_\rho) - \alpha \partial_\mu \partial_\rho] \mathfrak{D}'_{\rho\nu}(x-y) \\ + \int d^n \xi \Pi_{\mu\rho}(x-\xi) \mathfrak{D}'_{\rho\nu}(\xi-y) = -\delta^n(x-y). \quad (2.35)$$

Here color indices are suppressed and matrix multiplication is assumed; the gluon polarization

operator $\Pi_{\mu\nu}(x)$ is defined diagrammatically in Fig. 2. In the momentum representation, Eq. (2.35) becomes

$$[Z_3(g_{\mu\rho}q^2 - q_\mu q_\rho) + \alpha q_\mu q_\rho - \Pi_{\mu\rho}(q)]\mathfrak{D}'_{\rho\nu}(q) = 1. \quad (2.36)$$

Proceeding to the subtraction scheme relevant gauge identities will be obtained. Following the standard technique²³ we rewrite the unrenormalized partition function (2.2) in a factorized form

$$Z\{\eta, J\} = \Delta Z_0\{\eta, J\}, \quad (2.37)$$

$$\Delta = \frac{N(\beta)}{N_0(\beta)} \int \mathfrak{D}C \mathfrak{D}C^* \exp \left[- \int d^n x d^n y C^*(x) G^{-1} \left(x, y \left| \frac{\delta}{\delta J} \right. \right) C(y) \right], \quad (2.38)$$

where for later convenience the ghost propagator G in the presence of the external field $A_\mu^i(x)$ has been introduced,

$$G^{-1}(x, y | A) = \partial_\mu^x D_\nu^\mu(A) \delta^n(x - y), \quad (2.39)$$

$$D_\mu(A) \equiv \partial_\mu + g_0 T^i A_\mu^i. \quad (2.40)$$

Consider the result of infinitesimal gauge transformations

$$A_\mu^i(x) \rightarrow A_\mu^i(x) + D_\mu^{ij}(A) \epsilon^j(x), \quad (2.41a)$$

$$\psi(x) \rightarrow \psi(x) [1 - ig_0 \lambda^i \epsilon^i(x)], \quad (2.41b)$$

$$\bar{\psi}(x) \rightarrow \bar{\psi}(x) [1 + ig_0 \lambda^i \epsilon^i(x)], \quad (2.41c)$$

in the auxiliary functional $Z_0\{\eta, J\}$. Obviously the only gauge-noninvariant terms are sources and the gauge-fixing term $-(1/2\alpha_0)(\partial A)^2$ [see Eqs. (2.3)]. On the other hand, Eqs. (2.41) represent infinitesimal shifts in fields. Therefore, by familiar arguments one easily derives

$$\left[-ig_0 \frac{\delta}{\delta \eta(x)} \lambda^i \eta(x) - ig_0 \bar{\eta}(x) \lambda^i \frac{\delta}{\delta \eta(x)} + D_\nu^x \left(\frac{\delta}{\delta J} \right) \left(J^\nu(x) + \frac{1}{\alpha_0} \partial^\nu \partial^\mu \frac{\delta}{\delta J_\mu(x)} \right) \right] Z_0 = 0.$$

Upon action by $\Delta G(x, y | \delta/\delta J)$ it becomes

$$\left[\frac{1}{\alpha_0} \partial^\mu \frac{\delta}{\delta J_\mu(x)} \delta^n(x - y) + J^\mu(x) D_\mu^x \left(\frac{\delta}{\delta J} \right) G \left(x, y \left| \frac{\delta}{\delta J} \right. \right) \right] Z \Big|_{\bar{\eta}=\eta=0} = 0. \quad (2.42)$$

A functional derivative with respect to $J_\nu(z)$ gives

$$\left[\frac{1}{\alpha_0} \partial^\mu \frac{\delta}{\delta J_\mu(x)} \frac{\delta}{\delta J_\nu(y)} + D_\nu^x \left(\frac{\delta}{\delta J} \right) G \left(x, y \left| \frac{\delta}{\delta J} \right. \right) \right] Z \Big|_{J=\eta=0} = 0. \quad (2.43)$$

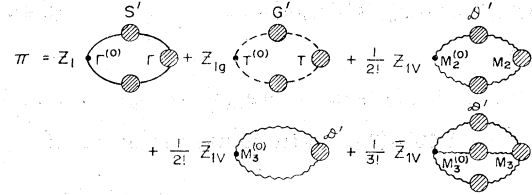


FIG. 2. Gluon polarization operator Π . Blobs designate full propagators S' , G' , \mathfrak{D}' and full vertices Γ , T , $M_{2,3}$. The Z 's stand for renormalization constants (see text).

After differentiating once we arrive at the desired identity

$$\partial_x^\mu \partial_x^\nu \mathfrak{D}'_{\mu\nu}(x - y) = -\alpha \delta^n(x - y), \quad (2.44)$$

where the definition (2.39) has been used and renormalized quantities according to (2.4) have been restored. Equation (2.44) is a generalization of the well-known non-Abelian gauge identity to the case of the nonzero temperature and nonvanishing Fermi densities. It suggests the following most general decomposition:

$$\mathfrak{D}'_{\mu\nu}(q) = (g_{\mu\nu}q^2 - q_\mu q_\nu) \frac{1}{q^4} d_1(q) + \alpha \frac{q_\mu q_\nu}{q^4} + (q_\mu Q_\nu + q_\nu Q_\mu) d_1(q) + \frac{Q_\mu Q_\nu}{q^4} d_2(q), \quad (2.45)$$

where

$$Q_\mu = \left\{ \begin{array}{l} Q_n = -(q^i q_i)^{1/2}, \\ Q_i = \frac{q_i q_n}{(q_i q_i)^{1/2}}, \quad i = 1, \dots, n-1 \end{array} \right\}$$

with properties $Q^2 = q^2$, $Q \cdot q = 0$. Observe that the presence of third and fourth terms in Eq. (2.45) are due to temperature and density effects.

Now we can fix the renormalization constant Z_3 . At zero temperature and zero density Eqs. (2.36) and (2.45) imply that the polarization operator is purely transverse

$$\Pi_0^{\mu\nu}(q) = (g^{\mu\nu}q^2 - q^\mu q^\nu) \Pi_0(q^2), \quad (2.46)$$

which suggests the choice [cf. Eq. (2.23a)]

$$Z_3 - 1 = \Pi_0(-M^2). \quad (2.47)$$

Evidently, the $1/\beta \neq 0$ or $\mu_A \neq 0$ induced effects generate in $\Pi_{\mu\nu}$ structure functions similar to $d_{1,2}$ in Eq. (2.45) which are expected to be devoid of primitive ultraviolet divergences.

Thus, the renormalized Dyson Eq. (2.36) may be rewritten as

$$[\mathfrak{D}_{\mu\nu}^{-1}(q) - \Pi_{\mu\nu}^R(q)]\mathfrak{D}'_{\rho\nu}(q) = 1, \tag{2.48}$$

where

$$\Pi_{\mu\nu}^R(q) = \Pi_{\mu\nu}(q) - (Z_3 - 1)(g_{\mu\nu}q^2 - q_\mu q_\nu). \tag{2.49}$$

Equation (2.46)–(2.49) will be used in Secs. III and IV.

III. PERTURBATIVE EXPANSION OF THE THERMODYNAMIC POTENTIAL

In this section a perturbative expansion in $\alpha(M) = g^2(M)/4\pi$ will be developed by means of a special reduction technique. The expansion is carried out for the fermion number $N_A(\mu) = -\delta\Omega/\delta\mu_A$ rather than the thermodynamic potential Ω itself. At zero temperature ($1/\beta=0$) the $\alpha(M)$ expansion for Ω will be easily reconstructed by a simple integration of the $N_A(\mu)$'s. In this approach the entire problem is reduced to the analysis of a single fermion propagator $S'(x, y)|_{y=x}$. This is an important virtue of our method over that of direct calculations of Ω .¹⁶ The reduction technique allows one to eliminate the chemical potential from the quark propagators and provides a constructive way to normal order the charge $\hat{O}_A(x)$.

First, fine points of the technique, such as treatment of singularities arising from discontinuous nature of the Fermi surface at $1/\beta=0$ and the significance of the quark mass definition

through Eqs. (23), will be exposed in the lowest and first nontrivial-order calculations.

Next the reduction technique will be applied to fourth-order terms in the perturbative expansion of N_A .

Finally, the resulting expressions will be further reduced to *bona fide* Feynman diagrams.

All analysis will be carried out in the $1/\beta=0$ limit. Special care is required for the limiting procedure. This important ingredient of the technique will be discussed in detail in Sec. III A.

A. Reduction of fermion densities in lower orders

The basis of our subsequent discussion is the expectation value of the fermion density \hat{O}_A ,

$$n_A(\mu) = \frac{\int d^n x \langle \bar{\psi}(x) i\gamma_n Z_2 O_A \psi(x) \rangle}{\beta V \langle 1 \rangle} - \left. \frac{\int d^n x \langle \bar{\psi}(x) i\gamma_n Z_2 O_A \psi(x) \rangle}{\beta V \langle 1 \rangle} \right|_{\mu_A=0}. \tag{3.1}$$

Henceforth, the volume V will be suppressed. In Eq. (3.1) the second term on the right-hand side ensures a vanishing fermion density at zero-chemical-potential limit. Alternatively, it accounts for the normal ordering of the charge density $\hat{O}_A(x)$. Since O_A 's are numerical matrices Eq. (3.1) may be expressed in terms of fermion propagators

$$n_A(\mu) = -\frac{1}{\beta} \sum_n \int \frac{d^{n-1}p}{(2\pi)^{n-1}} \text{Tr} \{ O_A i\gamma_n Z_2 [S'(p) - S'_0(p)] \} \Big|_{\mu_A=2\pi/\beta(m+1/2)} \tag{3.2}$$

By means of a standard trick, the sum \sum_n can be reduced to the contour integral along the lower (C_-) and upper (C_+) lips of the real axis in the complex p^n plane (see Fig. 3)

$$n_A(\mu) = -\int_{C_+} \frac{dp^n}{2\pi} \int \frac{d^{n-1}p}{(2\pi)^{n-1}} \eta(p^n) \text{Tr} \{ Z_2 O_A i\gamma_n [S'(p) - S'_0(p)] \}, \tag{3.3}$$

where

$$\eta(p^n) = (1 + e^{-ip^n\beta})^{-1}. \tag{3.4}$$

Recall that the fermion propagator $S'(p)$ is analytic in p^n with a cut along the imaginary axis. This is easy to verify in the perturbation theory. The general proof is straightforward and follows from the Lehmann spectral representation.²⁴ The contours C_\pm may be deformed *ab initio* reducing Eq. (3.3) to integrals along the imaginary axis $\text{Im}p^n > -\mu$ and the line $\text{Im}p^n = -\mu$. Notice that the contribution from the infinite circle can be ignored since $S'(p) - S'_0(p) \sim \mu/(p^n)^2$ as $|p^n| \rightarrow \infty$. However, a slightly different procedure will be

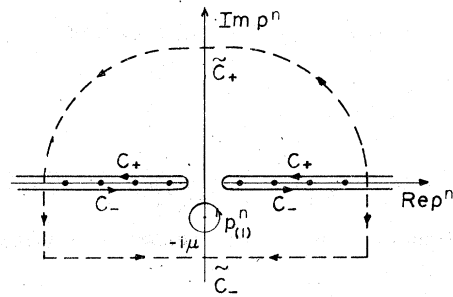


FIG. 3. Integration contours C_\pm, \tilde{C}_\pm in the complex energy plane p^n relevant for the evaluation of Eqs. (3.5), (3.8') (see text). The points $p^n = (2\pi/\beta)(m + \frac{1}{2})$ are indicated by dots on the real axis.

adopted. Namely, the C_{\pm} contours will be deformed *after* the interchange of the order of integration of internal momenta and the external momentum p^n . It is important to realize that contours C_{\pm} do not cross the imaginary axis. This is unlike the $\mu = 1/\beta = 0$ case when $S'_0(p)$ is analytic in the left- and right-half p^n planes connected through the mass gap $(-i\epsilon_p, +i\epsilon_p)$ with $\epsilon_p^2 = \vec{p}^2 + m^2$. The zero-temperature propagator $S'_{\mu \neq 0}(p)$ is not analytic at $p^n = 0$. This nonanalyticity is a potential source of singularities in $n_A(\mu)$. For this reason the p^n variable has been "latticized" via the nonzero-temperature formalism. The practical use of such a method will be more clear below. Here we only indicate that it allows one to smear out the Fermi surface smoothing the discontinuous character of the Fermi distribution at $1/\beta = 0$.

Being interested in the zero-temperature thermodynamic potential, we will examine Eq. (3.3) in the $1/\beta = 0$ limit

$$n_A = - \left\{ \left[\int_{C_{\pm}} \frac{d^n p}{(2\pi)^n} \eta(p^n) \text{Tr} O_A i\gamma_n Z_2 S'(p) \right] - [\mu = 0] \right\}_{1/\beta=0}. \quad (3.5)$$

Here the shorthand notation $[\mu = 0]$ has been introduced for the S'_0 term in Eq. (3.3). Now we will proceed to the perturbative evaluation of Eq. (3.5). In the lowest order $S'(p) = S(p)$ etc., and the first integral in Eq. (3.5) can be performed

$$n_A^{(2)} = Z_2^{(2)} n_A^{(0)} - \left\{ \int_{C_{\pm}} \frac{d^n p}{(2\pi)^n} \eta(p^n) \text{Tr} [O_A i\gamma_n S(p) \Sigma_R^{(2)}(p) S(p)] - [\mu = 0] \right\}_{1/\beta=0}. \quad (3.8)$$

We make use of Eq. (2.34a) to reduce the above expression to the form

$$n_A^{(2)} = - \left\{ \left[\int_{C_{\pm}} \frac{d^n p}{(2\pi)^n} \eta(p^n) \text{Tr} O_A i\gamma_n S(p) \tilde{\Sigma}^{(2)}(p) S(p) \right] - [\mu = 0] \right\}_{1/\beta=0}, \quad (3.8')$$

with

$$\tilde{\Sigma}(p) = \Sigma(p) - m(Z_m - Z_2). \quad (3.9)$$

Observe that the zero-temperature and zero-density counterpart $\tilde{\Sigma}_0$ of the above quantity vanishes on the mass shell [see Eqs. (2.19), (2.23)]

$$\tilde{\Sigma}_0(p) \Big|_{p=m} = 0. \quad (3.10)$$

Equation (3.10) will be consistently exploited throughout this section.

trivially by deforming the contour C_{\pm} to \tilde{C}_{\pm} simultaneously encircling the simple poles of $S(p)$ on the imaginary axis at $p_{(1)}^n = -i(\mu - \epsilon_p)$ as in Fig. 3. Recall that $\mu = \mu^A O_A$ and m are diagonal matrices and are, in general, different from the unit matrix in the flavor subspace. The same applies to the locations of the poles $p_{(1)}^n = -i(\mu - \epsilon_p)$. For clarity, matrix indices have been consistently suppressed. The integral along $\text{Im} p^n = -\mu$ exactly cancels the second term in Eq. (5), and one is left with

$$n_A^{(0)} = - \int \frac{d^{n-1} p}{(2\pi)^{n-1}} \left\{ \eta(p^n) \text{Tr} [O_A \gamma_n S(p)] \times (p^n - p_{(1)}^n) \right\}_{p^n = p_{(1)}^n, 1/\beta=0}. \quad (3.6)$$

After a simple integration one obtains

$$\Omega^{(0)} = -2D_F \int \frac{d^{n-1} p}{(2\pi)^{n-1}} \text{Tr} \{ (\mu - \epsilon_p) O(\mu - \epsilon_p) \} \quad (3.6')$$

where $\mu_a \equiv (O_A \mu^A)_{aa}$ and D_F is the dimension of the quark representation of the color group.

Let us turn to the next order of Eq. (3.5). One should expand Z_2 and $S'(p)$ via Eqs. (2.23) and (2.33)

$$Z_2 = 1 + Z_2^{(2)} + Z_2^{(4)} + \dots, \quad (3.7a)$$

$$S' = S + S \Sigma_R^{(2)} S + S \Sigma_R^{(2)} S \Sigma_R^{(2)} S + S \Sigma_R^{(4)} S + \dots \quad (3.7b)$$

Substituting Eqs. (3.7) into Eq. (3.5) one finds

The first term on the right-hand side of Eq. (3.8') is represented in Fig. 4. Here the quark self-energy insertion $\Sigma^{(2)}$ is determined by Eq. (2.34a) in which Z_1 , S' , Γ , and \mathfrak{D} had been replaced by their lowest-order approximations (see Fig. 1),

$$\Sigma^{(2)}(p) = \frac{1}{\beta} \sum_m \frac{d^{n-1} q}{(2\pi)^{n-1}} (-g\gamma_\mu \lambda^i) \times S(p-q) (-g\gamma_\nu \lambda^i) \mathfrak{D}_{ij}^m(q), \quad (3.11)$$

$$q = \left\{ q^n = \frac{2\pi}{\beta} m, \vec{q} \right\}.$$

Substituting Eqs. (3.9) and (3.11) into Eq. (3.8') and interchanging the order of integrations over p^n and q , one finds that the integrand has a double pole at $p_{(1)}^n = -i(\mu - \epsilon_p)$ and a simple pole at $p_{(2)}^n$

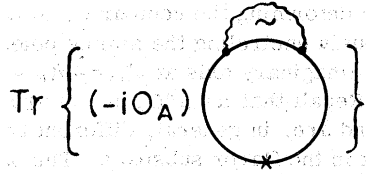


FIG. 4. Diagrammatic representation of the first term on right-hand side of Eq. (3.8'). The tilde in the self-energy insertion stands for the counterterm $m(Z_m - Z_2)^{(2)}$ [see Eq. (3.9)]. The vertex γ_n is designated by an \times .

$= q^n - i(\mu - \epsilon_{p-q})$, $\epsilon_{p-q} < \mu$. Similar to the treatment of Eq. (3.5) we deform the contour of integration C_{\pm} to \tilde{C}_{\pm} (see Fig. 3) picking up contributions from the poles $p_{(1,2)}^n$. The integral along $\text{Im} p^n = -\mu$ cancels the $[\mu=0]$ term in Eq (3.8'). The residues of the poles $p_{(1)}^n$ and $p_{(2)}^n$ are represented diagrammatically by Figs. 5(a), 5(b), and Fig. 5(c), respectively. Here the identity of $(d/dp^n)S(p) = S(p)\gamma_n S(p)$ has been employed in a diagrammatic form. It is not difficult to convince oneself that the diagrams in Figs. 5(b) and 5(c) are equal and of opposite sign.

To see this last point easily, we define the quantity

$$R(p) \equiv S(p)\gamma_n S(p) (p^n - p_{(1)}^n)^2, \quad (3.12)$$

which has the following simple properties:

$$R(p) \Big|_{p^n = p_{(1)}^n} = -S(p)(p^n - p_{(1)}^n) \Big|_{p^n = p_{(1)}^n}, \quad (3.13a)$$

$$\frac{dR(p)}{dp^n} \Big|_{p^n = p_{(1)}^n} = 0. \quad (3.13b)$$

The identity (3.13a) ensures the equality illustrated in Fig. 6. We apply this equality to Fig. 5(b) and make a subsequent change of the variable $\tilde{p} - \tilde{q} \rightarrow \tilde{p}$. Then the result stated above follows.

Thus, we are left with Fig. 5(a). A further ap-

plication of the identity (3.13a) yields

$$n_A^{(2)} = \int \frac{d^{n-1}p}{(2\pi)^{n-1}} \{ \eta'(p^n) \text{Tr}[O_A \tilde{\Sigma}^{(2)}(p)S(p)] \times (p^n - p_{(1)}^n) \Big|_{p^n = p_{(1)}^n, 1/\beta=0} \}. \quad (3.14)$$

Notice the appearance of the factor

$$\eta'(p_{(1)}^n) = \frac{d}{dp^n} \eta(p^n) \Big|_{p^n = -i(\mu - \epsilon_p)} \xrightarrow{1/\beta \rightarrow 0} i\delta(\mu - \epsilon_p), \quad (3.15)$$

which has support at a single point $p^n=0$. It should be clear, that a careful zero-temperature limiting procedure was essential for arriving at the correct result (3.14).

Now the equality (3.10) will be exploited. To this end first a relation between $\tilde{\Sigma}^{(2)}(p)$ and the Feynman self-energy $\Sigma_0^{(2)}(p)$ will be established. For real p the latter is given by a loop integral with an internal momentum q running along the real axis [cf. Eq. (3.11)]. Its integrand is analytic in q^n and has p^n -dependent poles at $q_{\pm}^n = p^n \pm i\epsilon_{p-q}$, $\text{Im} p^n = 0$, in upper- and lower-half planes, respectively. [see Fig. 7(a)]. When p^n acquires $\text{Im} p^n > 0$, and \tilde{p} and \tilde{q} are fixed, the pole q_{-}^n moves closer to the integration contour $\text{Im} p^n = 0$. The q_{-}^n reaches $C\{\text{Im} q^n = 0\}$ at $\text{Im} p^n = \epsilon_{p-q}$ and drags C upwards ($\epsilon_{p-q} < \text{Im} p^n$) without crossing it as it is shown in Fig. 7(a). The deformed contour $C'(p, \tilde{q})$ defines an analytic integral representation for

$$\tilde{\Sigma}_0^{(2)}(p) \Big|_{\text{Im} p^n = 0}$$

The $C'(p, \tilde{q})$ may be further deformed to the contour along the real axis C'_1 and a circle C'_2 around the pole q_{-}^n , $\text{Im} q^n > 0$ [see Fig. 7(b)]. The integral along C'_1 reproduces $\tilde{\Sigma}^{(2)}(p)$ in Eq. (3.14), whereas the C'_2 integral is equal to the residue of the pole q_{-}^n with the opposite sign. It remains to recall Eq. (3.10) to arrive at the result exhibited in Fig. 8. Thus, Eq. (3.14) reduces to

$$n_A^{(2)}(\mu) = g^2 D_F C_F \int \prod_{i=1}^2 \frac{d^{n-1}p_i}{(2\pi)^{n-1}} \text{Tr} \{ \delta(\mu - \epsilon_1) O(\epsilon_1 - \epsilon_2) \mathfrak{D}_{\mu\nu}(p_1 - p_2) O_A \gamma^\mu S_0(p_1) \gamma^\nu S_0(p_2) (p_1 - i\epsilon_1)(p_2 - i\epsilon_2) \}, \quad (3.16)$$

$$p_{1,2}^n = i\epsilon_{1,2}, \quad \epsilon_{1,2} \equiv \epsilon_{p_{1,2}},$$

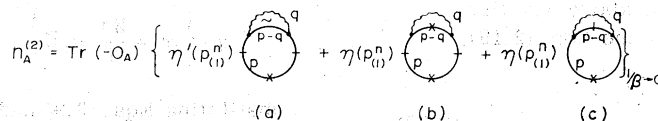


FIG. 5. Diagrammatic evaluation of Eq. (3.8'). Barred lines represent residues of the fermion propagators, $+_p = S(p)(p^n - p_{(1)}^n) \Big|_{p^n = p_{(1)}^n}$, $p_{(1)}^n = -i(\mu - \epsilon_p)$. The integrations over the corresponding loop momenta p are restricted to the spatial phase space with volume element $d^{n-1}p/(2\pi)^{n-1}$.

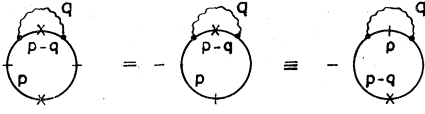


FIG. 6. Equation resulting from the application of Eqs. (3.12), (3.13a) to the diagram in Fig. 5(b).

where D_F has already been defined in Eq. (3.6'), whereas C_F is the eigenvalue of the first Casimir operator in the quark representation of the color group

$$(\lambda^i \lambda^i)_{ab} = C_F \delta_{ab}, \quad \text{Tr}(\lambda^i \lambda^i) = C_F D_F. \quad (3.17)$$

Equation (3.16) can be easily integrated with respect to μ_A to find the second-order correction to the thermodynamic potential

$$\Omega^{(2)} = \frac{1}{2} g^2 D_F C_F \text{Tr} \int \prod_{i=1}^2 \frac{d^{n-1} p_i}{(2\pi)^{n-1} \epsilon_i} \theta(\mu - \epsilon_i) \times \left[1 + \frac{2m^2}{(p_1 - p_2)^2} \right]. \quad (3.18)$$

This is a well-known result which accounts for one gluon exchange scattering of quarks (cf. Fig. 9).

B. Reduction of fermion densities in higher orders

It will be helpful to recapitulate two major elements of the reduction technique employed in a restricted form in the previous subsection:

1. Rearrangement of the perturbative expansion of Eq. (3.5) into terms with a different number of free fermion propagators through a partial disentanglement of renormalization constants $Z_{1,2}$ present in Eqs. (2.33), (2.34) either in an explicit or in an implicit form. It is important that in the above rearrangement the *mass term* $m(Z_m - Z_2)$ in Eq. (2.34a) be left intact for the subsequent use of the on-mass-shell condition (3.10). The application of this step to Eq. (3.5) yielded Eq. (3.8').

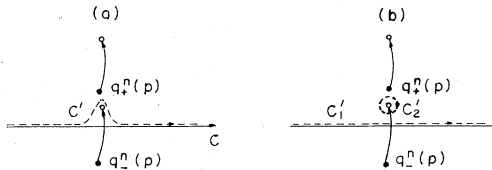


FIG. 7. (a) Points $q_1^n(p) = p^n + i\epsilon_{p-q}$ indicate the location of p^n -dependent poles in the integrand of $\Sigma_0^{(2)}(p)$ [cf. Eq. (3.11)]. When p^n acquires $\text{Im} p^n > 0$, the lower pole q_2^n approaches the q^n integration contour C and drives it upwards to the position C' ($\text{Im} q_2^n > 0$). (b) Contour C' in (a) is deformed to $C'_1 \cup C'_2$.

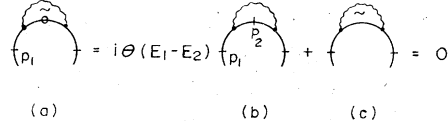


FIG. 8. The relation at $1/\beta = 0$ between the Feynman self-energy $\Sigma_0^{(2)}(p_1)|_{p_1^n = i\epsilon_p}$ given by (a) and its counterpart (c).

2. Interchange of the order of integration over the external loop momentum p^n and those of internal loops. This step reduces the p^n integral along C_\pm to a sum of residues of first- and higher-order poles and a residual integral along \tilde{C}_\pm , which cancels the term $[\mu = 0]$. Further simplification of the resulting expression is achieved through simple identities like Eq. (3.13) and the on-mass-shell condition (3.10). The application of this step to Eq. (3.8') yielded Eq. (3.16).

We proceed to the analysis of fourth-order corrections to fermion densities (3.5). For clarity the first step will be carried out in two stages. To begin with the $Z_2 S'$ in Eq. (3.5) will be expanded according to Eqs. (3.7), and only the terms containing $Z_{1,2}$ explicitly will be disentangled; the renormalized propagator S' and the vertex function Γ in $\Sigma_R^{(4)}$ will be replaced by their lowest-order approximations $S'^{(2)}$ and $\Gamma^{(2)}$, respectively. The same approximation is invalid for the gluon propagator \mathfrak{D}' since it gives rise to infrared divergences. Therefore, the \mathfrak{D}' will be left intact, and the analysis of the corresponding term will be deferred to Sec. IV. After simple rearrangements one arrives at

$$(Z_2 S')^{(4)} = -Z_2^{(2)} S \tilde{\Sigma}^{(2)} S + S \tilde{\Sigma}^{(2)} S \tilde{\Sigma}^{(2)} S + S [\Sigma^{(4)} - m(Z_m - Z_2)^{(4)}] S, \quad (3.19)$$

$$\Sigma^{(4)} = Z_1^{(2)} \Sigma^{(2)} + [\Gamma^{(0)} S'^{(2)} \Gamma^{(0)} \mathfrak{D}] + [\Gamma^{(0)} S \Gamma^{(2)} \mathfrak{D}] + [\Gamma^{(0)} S \Gamma^{(0)} \mathfrak{D}']^{(4)}. \quad (3.20)$$

The first step of the reduction will be completed by a disentanglement of $S'^{(2)}$ and $\Gamma^{(2)}$ in Eq. (3.20):

$$S'^{(2)} = -Z_2^{(2)} S + S \tilde{\Sigma} S, \quad (3.21a)$$

$$\Gamma^{(2)} = Z_1^{(2)} \Gamma^{(0)} + \Gamma_B^{(2)}, \quad (3.21b)$$

where $\Gamma_B^{(2)}$ is the unrenormalized counterpart of the vertex $\Gamma^{(2)}$. Equation (3.19) becomes

$$(Z_2 S')^{(4)} = (Z_2 S')_{a+b+c+d+e}^{(4)} \quad (3.22)$$

$$\Omega^{(2)} = -\text{Tr} \left\{ \theta(\mu - E_1) \theta(E_1 - E_2) \left(\text{loop} \right) \right\} = \text{Tr} \left\{ \theta(\mu - E_1) \theta(E_1 - E_2) \left\langle \frac{p_2}{p_1} \frac{p_2}{p_1} \right\rangle \right\}$$

FIG. 9. Second-order correction to the thermodynamic potential due to one-gluon exchange. Barred lines are for residues of $S_0(p)$, i.e., $\bar{+}_p = S_0(p)(p^n - i\epsilon_p)|_{p^n = i\epsilon_p}$.

with

$$(Z_2 S')_a^{(4)} = -S [m(Z_m - Z_2)^{(4)} + Z_2^{(2)} \bar{\Sigma}^{(2)} + (Z_2 - 2Z_1)^{(2)} \Sigma^{(2)}] S, \quad (3.23a)$$

$$(Z_2 S')_b^{(4)} = S(\bar{\Sigma}^{(2)} S \bar{\Sigma}^{(2)}) S, \quad (3.23b)$$

$$(Z_2 S')_c^{(4)} = S(\Gamma^{(0)} S \bar{\Sigma} \Gamma^{(0)} \mathcal{D}) S, \quad (3.23c)$$

$$(Z_2 S')_d^{(4)} = S(\Gamma^{(0)} S \Gamma_B^{(2)} \mathcal{D}) S, \quad (3.23d)$$

$$(Z_2 S')_e^{(4)} = S(\Gamma^{(0)} S \Gamma^{(0)} \mathcal{D}')^{(4)} S. \quad (3.23e)$$

Owing to the decomposition (3.22) it is convenient to represent the fourth-order correction $n_A^{(4)}$ to fermion densities (3.5) as a sum of terms

$$n_A^{(4)} = n_A^{(a)} + n_A^{(b)} + n_A^{(c)} + n_A^{(d)} + n_A^{(e)}, \quad (3.24)$$

with

$$n_A^{(S)} = - \left\{ \left[\int_{C_{\pm}} \frac{d^n p}{(2\pi)^n} \eta(p^n) \text{Tr} O_A i \gamma_n (Z_2 S'(p)) \right]_{(S)} \right. \\ \left. - [\mu=0]_{(S)} \right\}_{1/\beta=0}, \quad S = a, b, \dots \quad (3.25)$$

In curly brackets the $[\mu=0]_{(S)}$ designates the zero-fermion-density counterpart of the preceding term.

The second step of reduction will be carried out separately for each term of Eq. (3.24). The reduced form of the first term $n_A^{(a)}$ immediately follows from the previous analysis. Indeed, it is sufficient to repeat the steps leading from Eq. (3.8') to Eq. (3.14) to arrive at the result in Fig. 10.

The analysis of the contribution $n_A^{(b)}$ is straightforward although slightly tedious. In the process of deforming the contour C_{\pm} to \bar{C}_{\pm} , one encounters two first-order poles at $p^n = q^n - i(\mu - \epsilon_{p-q})$, $p^n = k^n - i(\mu - \epsilon_{p-k})$ and a third-order pole at $p^{(n)} = -i(\mu - \epsilon_p)$, where q and k are momenta of internal loops of two self-energy insertions $\bar{\Sigma}^2$. The residues of the poles are evaluated diagrammatically in Fig. 11 via the identity $(d/dp^n)S(p) = S(p)\gamma_n S(p)$. Those diagrams, which identically vanish due to Eq. (3.13b), have been dropped.

The above result may be simplified as follows. Firstly, the last two diagrams on the third line cancel. Indeed, it is easy to verify that

$$\frac{d^2}{d(p^n)^2} [S(p)(p^n - p_{(1)}^n)]_{p^n=p_{(1)}^n} \\ = \frac{d^2}{d(p^n)^2} [S(p)\gamma_n S(p)(p^n - p_{(1)}^n)]_{p^n=p_{(1)}^n},$$

$$p_{(1)}^n = -i(\mu - \epsilon_p).$$

Secondly, we apply the identity (3.13a) (cf. Fig. 6) and notice that some diagrams become topologically identical, e.g., the first two diagrams on the second line etc. After these simplifications

one arrives at Fig. 12.

The reduced form of the term $n_A^{(c)}$ is exhibited in Fig. 13. The contribution is due to two second-order poles at $p^n = -i(\mu - \epsilon_{p-k})$ and $p^n = q^n - i(\mu - \epsilon_{p-q})$ and one first-order pole at $p^n = q^n + k^n - i(\mu - \epsilon_{p-q-k})$, where q and k are internal-loop momenta.

The same reduction when applied to $n_A^{(d)}$ and $n_A^{(e)}$ leads to the results shown in Fig. 14. In the derivation of $n_A^{(e)}$ Furry's theorem has been employed, namely, fermion loops with three attached gluon lines have been set to zero, in particular, $[\mu=0]_{(e)} = 0$. The simplicity of the above forms is due to the topological equivalence of the resulting diagrams which leads to many cancellations explicitly demonstrated in the case of $n_A^{(e)}$.

Finally, we combine Figs. 10, 12-14. One discovers the same type of cancellations, e.g., the third diagram on the first line in Fig. 12 cancels the first diagram on the second line in Fig. 13. The cancellation is easy to see by turning the latter's upper "rainbow" upside down. The net result is exhibited in Fig. 15. It determines a full fourth-order correction $n_A^{(4)}$ to the fermion densities n_A .

Observe that terms proportional to $\eta(p^n)$ disappeared altogether and only those with derivatives of $\eta(p^n)$, namely $\eta'(p_{(1)}^n)$ and $\eta''(p_{(1)}^n)$ survived. These are singular at $1/\beta=0$. We reemphasize that the presence of these singular factors proves the necessity of very careful treatment of zero-temperature limits.

C. Reduction of fermion densities to Feynman diagrams

In this subsection the final stage of the reduction will be completed. All diagrams in Fig. 15 will be expressed in terms of *bona fide* Euclidean Feynman diagrams. In what follows we will set $1/\beta=0$ wherever it does not give rise to any singularities. Furthermore, the Feynman gauge will be adopted for convenience, i.e., in the gluon propagator the gauge parameter α will be set equal to one [see Fig. 1(b)]. Observe that for fourth-order calculations the renormalization of α by Eq. (2.4d) is unnecessary since the lower-order result, Eq. (3.16) is gauge invariant.

The method employed below is a generalization

$$n_A^{(a)} = -\text{Tr} O_A \eta'(p_{(1)}^n) \left\{ \text{Diagram 1} \right. \\ \left. + \text{Diagram 2} \right\} \\ \text{Diagram 1: } 2(Z_2 - Z_1)^{(2)} \\ \text{Diagram 2: } m [(Z_m - Z_2)^{(4)} + (Z_m - Z_2)^{(2)} (Z_2 - 2Z_1)^{(2)}]$$

FIG. 10. Fourth-order correction $n_A^{(a)}$ to fermion densities [see Eq. (3.25)].

$$\begin{aligned}
 n_A^{(b)} = & -\text{Tr } O_A \eta(\rho_{(1)}^n) \left\{ \text{Diagram 1} + \text{Diagram 2} \right\} \\
 & -\text{Tr } O_A \eta(\rho_{(1)}^n) \left\{ \text{Diagram 3} + \text{Diagram 4} + \text{Diagram 5} + \right. \\
 & \left. + \text{Diagram 6} + \text{Diagram 7} + \frac{1}{2} \text{Diagram 8} + \frac{1}{2} \text{Diagram 9} \right\} \\
 & -\text{Tr } O_A \eta'(\rho_{(1)}^n) \left\{ \text{Diagram 10} + \text{Diagram 11} + \text{Diagram 12} \right\} + \\
 & -\frac{1}{2} \text{Tr } O_A \eta''(\rho_{(1)}^n) \text{Diagram 13}
 \end{aligned}$$

$$\begin{aligned}
 \text{Diagram 1} &= \frac{d}{d\rho^n} \left[S(\rho) (\rho^n - \rho_{(1)}^n) \right]_{\rho^n = \rho_{(1)}^n} \\
 \text{Diagram 2} &= \frac{d^2}{d(\rho^n)^2} \left[S(\rho) (\rho^n - \rho_{(1)}^n) \right]_{\rho^n = \rho_{(1)}^n} \\
 \text{Diagram 3} &= \frac{d^2}{d(\rho^n)^2} \left[S(\rho) \gamma_n S(\rho) (\rho^n - \rho_{(1)}^n)^2 \right]_{\rho^n = \rho_{(1)}^n}
 \end{aligned}$$

FIG. 11. (a) Fourth-order correction $n_A^{(b)}$ to fermion densities [see Eq. (3.25)]. Rules are as in Figs. 4, 5 and further graphical notation is explained in (b). (b) Notations used in (a) with $p_{(1)} = -i(\mu - \epsilon_p)$.

of the derivation of Eq. (3.16) from Eq. (3.14) based on the relation between the $\tilde{\Sigma}^{(2)}(p)$ and the Feynman self-energy $\tilde{\Sigma}_0^{(2)}(p)$.

Let us begin with the diagram in Fig. 15(f). Its Euclidean Feynman counterpart is usually defined for real external momenta p (see Fig. 16). Applying the arguments exemplified in Fig. 7 to the internal momentum k^n , one derives the relation in Fig. 16 where the momentum q^n of the second internal loop is real, whereas that of the external one is complex, $p^n = i\epsilon_p$, $p^2 = m^2$. Notice that in Fig. 15(a) the self-energy insertion with an internal-loop momentum k defines a bona fide Feynman diagram $\tilde{\Sigma}_0^{(2)}(p - q)$ whose external momentum $p^n - q^n$ is analytically continued to complex values. We will examine diagrams (a) and (b) in Fig. 15 separately.

In the former case one could deform the q^n integration contour from C to C' as in Fig. 7. How-

$$\begin{aligned}
 n_A^{(b)} = & -\text{Tr } O_A \eta(\rho_{(1)}^n) \left\{ \text{Diagram 1} + \text{Diagram 2} - 2 \text{Diagram 3} \right. \\
 & \left. - \text{Diagram 4} - \text{Diagram 5} - \text{Diagram 6} \right\} \\
 & + \text{Tr } O_A \eta'(\rho_{(1)}^n) \left\{ 2 \text{Diagram 7} + \text{Diagram 8} \right\} + \frac{1}{2} \text{Tr } O_A \eta''(\rho_{(1)}^n) \text{Diagram 9}
 \end{aligned}$$

FIG. 12. Simplified form of Fig. 11.

$$\begin{aligned}
 n_A^{(c)} = & \text{Tr } O_A \left\{ \eta(\rho_{(1)}^n) \text{Diagram 1} + \eta(\rho_{(1)}^n) \text{Diagram 2} + \eta'(\rho_{(1)}^n) \text{Diagram 3} - \eta'(\rho_{(1)}^n) \text{Diagram 4} \right\} \\
 & -\text{Tr } O_A \eta(\rho_{(1)}^n) \left\{ 2 \text{Diagram 5} + \text{Diagram 6} + \text{Diagram 7} + \text{Diagram 8} \right\}
 \end{aligned}$$

FIG. 13. Fourth-order correction $n_A^{(c)}$ to fermion densities [see Eq. (3.25)]. Rules are as in Fig. 11.

ever, special care has to be exercised since $\tilde{\Sigma}_0(p - q)$, $p^n = i\epsilon_p$ has two cuts along the q^n imaginary axis with a gap $[i(\epsilon_p - \epsilon_{p-q}), i(\epsilon_p + \epsilon_{p-q})]$ between them. Therefore, the contour C' should pass above the second-order pole at $q^n = q_2^n = i(\epsilon_p - \epsilon_{p-q})$ and, furthermore, pass through the gap without crossing the cuts as shown in Fig. 17. The result defines a bona fide Feynman diagram, exhibited in Fig. 18(a). It is now clear that by deforming the contour C' to C , one picks up the residue of the second-order pole [see Fig. 18(c)] as well as a contribution from the discontinuity across the cut $(0, q_2^n)$ of the self-energy subdiagram $\Sigma_0^{(2)}(p - q)$ [see Fig. 18(d)]. The former has been evaluated using Eq. (3.10).

Returning to Fig. 16(b) one easily derives the relation in Fig. 19. The integral representation of the Feynman diagram in Fig. 19(a) is such that the q^n integration contour C' passes above the simple pole at $q^n = q_1^n$ with $q_1^n = p_1^n - p_2^n \mp i\epsilon_{p_1 - p_2 - q}$ and the double pole at $q^n = q_2^n$, $q_2^\pm = p_1^\pm \pm i\epsilon_{p_1 - q}$, leaving the upper poles q_{1+} and q_{2+} on the left as in Fig. 7(a). Deforming C' to the real axis (C) one immediately recovers the result in Fig. 19. The equations in Figs. 16, 18, and 19 determine the diagram in Fig. 15(f) which may be combined with Figs. 15(c), 15(d) in a concise form. Indeed, using Eq. (3.13b) and Fig. 8 one can reduce Fig. 15(c) as it is shown in Fig. 20. Observe that Figs. 18(c), 19(d), 19(e), and 19(f), 19(g) are topologically equivalent to Figs. 20(a), 15(d), and 20(b), respectively. Furthermore, it is easy to see that the diagrams in Figs. 18(d) and 19(c), arising from the two-particle unitarity discontinuities, cancel. Hence, the equation in Fig. 21 follows.

The reduction of Fig. 15(g) can be performed in the same manner. The necessary steps are exhibited diagrammatically in Fig. 22 and the net

$$\begin{aligned}
 n_A^{(d)} = & \text{Tr } O_A \eta'(\rho_{(1)}^n) \left\{ \text{Diagram 1} + \text{Diagram 2} \right\} \\
 n_A^{(e)} = & \text{Tr } O_A \left\{ \eta'(\rho_{(1)}^n) \text{Diagram 3} + \eta(\rho_{(1)}^n) \text{Diagram 4} - \eta(\rho_{(1)}^n) \text{Diagram 5} \right\}
 \end{aligned}$$

FIG. 14. Fourth-order corrections $n_A^{(d,e)}$ to fermion densities [see Eq. (3.25)]. Rules are as in Fig. 11.

$$\begin{aligned}
 n_A^{(4)} = & -\text{Tr} O_A \eta'(\rho_{(1)}^n) \left\{ \text{(a)} \quad \text{m} [(Z_m - Z_2)^{(4)} + (Z_m - Z_2)^{(2)} (Z_2 - 2Z_1)^{(2)}] + \text{(b)} \quad 2(Z_2 - Z_1)^{(2)} \right\} \\
 & + \text{Tr} O_A \left\{ \eta'(\rho_{(1)}^n) \text{(c)} + \eta'(\rho_{(1)}^n) \text{(d)} + \frac{1}{2} \eta''(\rho_{(1)}^n) \text{(e)} \right\} \\
 & + \text{Tr} O_A \eta'(\rho_{(1)}^n) \left\{ \text{(f)} + \text{(g)} + \text{(i)} + \text{(h)} \right\}
 \end{aligned}$$

FIG. 15. Full fourth-order corrections to fermion densities. Rules are as in Fig. 11.

result is summarized in Fig. 23.

Finally, the reduced forms of the remaining diagrams, Figs. 15(i) and 15(h), can be obtained in a similar fashion. They are presented in Figs. 24, 25.

We substitute the results of our analysis of Figs. 21, 23–25 into the expression for the fermion densities, Fig. 15. It is easy to see that due to the mass-shell condition $\Sigma_0^{(4)}(m) = m(Z_m - Z_2)^{(4)}$ the terms in Figs. 21(d), 23(a), 24(a), and 25(a) are cancelled by $m(Z_m - Z_2)^{(4)} - m(Z_m - Z_2)^{(2)} Z_1^{(2)}$, whereas the remaining renormalization constants render the Abelian vertex \times in Fig. 21(c) and the gluon-quark vertex in Figs. 23(c), 24(b), renormalized. After a trivial integration with respect to μ_A , and using Eq. (2.15), we obtain a diagrammatic expansion for the fourth-order correction $\Omega^{(4)}$ of the zero-temperature thermodynamic potential.

To facilitate the subsequent discussion $\Omega^{(4)}$ has been broken up into three parts

$$\Omega^{(4)} = \Omega_1^{(4)} + \Omega_2^{(4)} + \Omega_3^{(4)} \tag{3.26}$$

and represented diagrammatically in Figs. 26–28. Recall that they arose from topologically distinct diagrams determined by Eqs. [(3.23b), (3.23d)], (3.23c), (3.23e), respectively. Correspondingly $\Omega_{1,2,3}^{(4)}$ will be referred to as the quark self-energy, quark-gluon vertex, and gluon self-energy corrections.

It is interesting that all diagrams except those in Figs. 26(a), 26(d), 26(e), are given by ordinary Feynman scattering amplitudes of quarks. Since

$$\text{(a)} = \text{(b)} - i\theta (E_1 - E_2) \text{(c)}$$

FIG. 16. Reduction of Fig. 15. The circle on the fermion propagators in (a) indicates that the integration in k^n is along a contour going around the pole $k_-^n = p_1^n - q^n - i\epsilon_{p-q-k}$ from above rather than from below, i.e., just like C' in Fig. 7(a).

the quarks form a Fermi sea, only exchange (backward) scatterings are allowed. However, in addition, there are residual diagrams [see Figs. 26(a), 26(d), 26(e)] which will turn out to be crucial to render $\Omega^{(4)}$ regular at the zero-quark-mass limit.

In conclusion, we must emphasize that in the derivation of Eq. (3.26) the space-time dimension n has not been specified. Therefore, all infrared singularities in various terms of Eq. (3.26) are automatically regulated. The resolution of the problems encountered in taking the physical limit $n = 4$ forms a part of the subject of the next section.

IV. FOURTH-ORDER CORRECTIONS TO THE THERMODYNAMIC POTENTIAL

Analytic expressions for the fourth-order corrections to the thermodynamic potential will be given. Further, they will be evaluated exactly in the zero-quark-mass limit, $m = 0$.

All calculations will be carried out for an arbitrary space-time dimension n . Infrared and mass singularities of individual diagrams in Figs. 26–28 will be exhibited in the form of first- and second-order poles at $n = 4$. The cancellation of these singularities at $m = 0$ for each subset of diagrams $\Omega_i^{(4)}$, $i = 1, 2, 3$, as $n \rightarrow 4$ will be demonstrated in de-

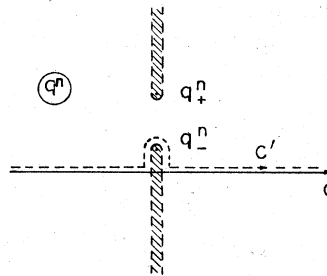


FIG. 17. Cuts of the self-energy $\tilde{\Sigma}_0^{(2)}(p-q)|_{p^n = i\epsilon_p}$ are shown by dashed strips along the imaginary axis in the q^n plane. The cuts end at $q_{\pm}^n = i(\epsilon_p \pm \epsilon_{p-q})$, $\epsilon_p > \epsilon_{p-q}$.

tail. The result agrees with the general assertion made in the Introduction that the thermodynamic potential of the ground state is devoid of infrared and mass singularities.

In conclusion, various definitions of the renormalized coupling and its gauge dependence will be discussed. Furthermore, standard renormalization-group arguments will be advanced to motivate the optimal choice of the subtraction point

M . In this context the absence of mass singularities is crucial for a valid perturbation expansion even for $m_a \neq 0$, $m_a \ll M$.

A. Quark self-energy correction $\Omega_1^{(4)}$

Using the Feynman rules of Fig. 1 with $\alpha = 1$, one can easily write down analytic expressions for the diagrams in Fig. 26:

$$\Omega_{1a}^{(4)} = \frac{1}{2} g^4 \text{Tr} \int \prod_{a=1}^3 \frac{d^{n-1} p_a}{(2\pi)^{n-1}} \left[\frac{\delta(\mu - \epsilon_1) \theta(\mu - \epsilon_2) \theta(\mu - \epsilon_3) \gamma^\nu \lambda^i(\not{p}_1 + m) \gamma^\mu \lambda^j(\not{p}_2 + m) \gamma_\mu \lambda^j(\not{p}_1 + m) \gamma_\nu \lambda^i(\not{p}_3 + m)}{(p_1 - p_2)^2 (p_1 - p_3)^2} \frac{1}{2i\epsilon_1} \frac{1}{2i\epsilon_2} \frac{1}{2i\epsilon_1} \frac{1}{2i\epsilon_3} \right], \quad (4.1a)$$

$$\Omega_{1b}^{(4)} = -g^4 \text{Tr} \int \prod_{a=1}^2 \frac{d^{n-1} p_a}{(2\pi)^{n-1}} \theta(\mu - \epsilon_a) \left[\frac{\not{p}_1 + m}{2i\epsilon_1} \gamma^\mu \lambda^i(\not{p}_2 + m) \gamma_\mu \lambda^i(\not{p}_1 + m) \Gamma_{\text{on}}^{(2)}(p_1, p_1 | 0) \right] \frac{1}{(p_1 - p_2)^2} \quad (4.1b)$$

with [cf. Eqs. (2.13), (2.29)]

$$\Gamma_{\text{on}}^{(2)}(p_1, p_1 | 0) = \left(\frac{d}{dp^n} \Sigma_0^{(2)}(p_1) - \gamma_n \Sigma_1^{(2)}(-M^2) \right)_{p_1^2 = m^2},$$

$$\Omega_{1c}^{(4)} = -\frac{1}{2} g^4 \text{Tr} \int \prod_{a=1}^2 \frac{d^{n-1} p_a \theta(\mu - \epsilon_a)}{(2\pi)^{n-1}} \int \frac{d^n q}{(2\pi)^n} \times \left\{ \frac{(\not{p}_1 + m) \gamma^\mu \lambda^i}{2i\epsilon_1} \frac{(\not{p}_1 - \not{q} + m) \gamma^\nu \lambda^j(\not{p}_2 + m) \gamma_\nu \lambda^j(\not{p}_1 - \not{q} + m) \gamma_\mu \lambda^i}{[(p_1 - q)^2 - m^2] (2i\epsilon_2) q^2 [(p_1 - q)^2 - m^2] (p_1 - p_2 - q)^2} \right\}, \quad (4.1c)$$

$$\Omega_{1d}^{(4)} = i g^4 \text{Tr} \int \prod_{a=1}^3 \frac{d^{n-1} p_a \theta(\mu - \epsilon_a)}{(2\pi)^{n-1}} \left\{ \frac{(\not{p}_1 + m) \gamma^\mu \lambda^i(\not{p}_2 + m) \gamma_\mu \lambda^i}{2i\epsilon_1} \frac{1}{\left[\frac{(\not{p}_1 + m)}{p_1^n + i\epsilon_1} \right]_{p_1^n = i\epsilon_1}} \frac{\gamma^\nu \lambda^j(\not{p}_3 + m) \gamma_\nu \lambda^j}{2i\epsilon_3} \right\} \frac{1}{(p_1 - p_2)^2 (p_1 - p_3)^2}, \quad (4.1d)$$

$$\Omega_{1e}^{(4)} = i g^4 \text{Tr} \int \prod_{a=1}^3 \frac{d^{n-1} p_a \theta(\mu - \epsilon_a)}{(2\pi)^{n-1}} \left[\frac{(\not{p}_1 + m) \gamma^\mu \lambda^i(\not{p}_2 + m) \gamma_\mu \lambda^i}{2i\epsilon_1} \frac{1}{2i\epsilon_2} \times \frac{(\not{p}_1 + m) \gamma^\nu \lambda^j(\not{p}_3 + m) \gamma_\nu \lambda^j}{2i\epsilon_3} \right] \frac{1}{(p_1 - p_2)^2} \frac{(p_1^n - p_3^n)}{(p_1 - p_3)^4}. \quad (4.1e)$$

Note that in the above equations the trace applies to all indices, i.e., flavor (a), color (i), and Dirac (α). Also recall that $\mu \equiv \mu^A O_A$ and m are diagonal matrices with unequal elements (μ_a, m_a) in the flavor subspace if the flavor symmetry is broken. Clearly, the above expressions are reducible to a direct sum of contributions due to different flavors; quarks of a definite flavor propagate in a given diagram. The trace over color indices may

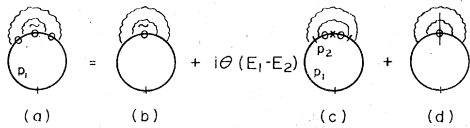


FIG. 18. Relation between the Feynman diagram (a) and its counterpart (b). (c) and (d) are contributions arising from the residue of the second-order pole at $q^n = q_+^n$, and from the discontinuity across the cut $(0, q_+^n)$, respectively.

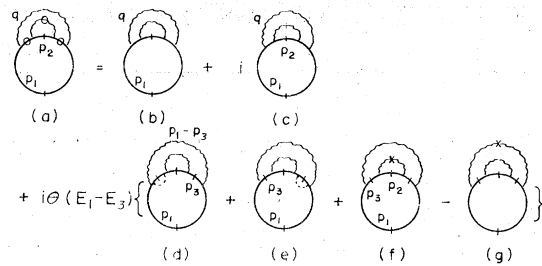


FIG. 19. Relation between the Feynman diagram (a) and its counterpart in Fig. 16(b). Contributions due to residues of (c) a simple pole of the gluon propagator $D_{\mu\nu}(p_1 - p_2 - q)$ at $q^n = p_1^n - p_2^n - i\epsilon_{p_1 - p_2 - q}$ and (d)-(g) double pole of fermion propagators $S^2(p_1 - q)$ at $q^n = p_1^n - i\epsilon_{p_1 - q}$. Rules are as in Fig. 11 and in addition

$$\text{---} \times \text{---} = \mathfrak{D}_{\mu\nu}(p) (p^n - i|\vec{p}|)_{p^n = i|\vec{p}|},$$

$$\text{---} \times \text{---} = \frac{d}{dp^n} \mathfrak{D}_{\mu\nu}(p).$$

The Feynman gauge is assumed.

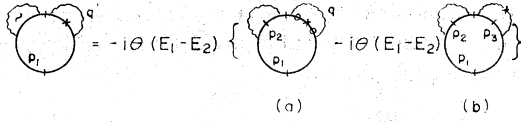


FIG. 20. (a) Feynman counterpart of the left-hand side diagram. (b) Residue of the double pole at $q_1^2 = p_1^2 - i\epsilon_{p-q}$, $p_1^2 = i\epsilon_1$ due to the vertex \times subdiagram.

be easily taken by Eq. (3.17).

It is not difficult to convince oneself that from Eqs. (4.1) only Eq. (4.1b) is infrared singular due to the presence of the on-mass-shell vertex Γ_{on} . This singularity is expected to cancel with the infrared singularity of Fig. 27(a). However, in the zero quark mass limit, $m=0$, the sum of Eqs. (4.1) by themselves will be found to be regular.

Now we set $m=0$ in Eqs. (4.1) and proceed to the analytic evaluation of the resulting expression. For the reader's convenience we will write down for n dimensions some well-known identities for Dirac matrices and some integration formulas which will be used throughout this section

$$\gamma^\mu \gamma^\nu + \gamma^\nu \gamma^\mu = 2g^{\mu\nu}, \quad g^{\mu\nu} g_{\mu\nu} = \delta_\nu^\mu = n, \quad (4.2a)$$

$$\text{Tr} \gamma^\mu \gamma^\nu = 4g^{\mu\nu}, \quad (4.2b)$$

$$\gamma^\mu \not{p} \gamma_\mu = -(n-2)\not{p}, \quad (4.2c)$$

$$d^{n-1}p = p^{n-2} dp \prod_{m=1}^{n-2} \sin^{m-1} \theta_m d\theta_m, \quad (4.3a)$$

$$\int \prod_{a=1}^2 \frac{d^{n-1}p_a \theta(\mu - \epsilon_a)}{(2\pi)^{n-1} 2\epsilon_a} (2p_1 p_2)^m = \frac{(\mu^2)^{m+n-2}}{(4\pi)^{n-1} \sqrt{\pi}} \frac{2^{n+2m-3} \Gamma(\frac{1}{2}n+m-1)}{\Gamma(n-1/2)\Gamma(n+m-1)(n+m-2)},$$

$$(p_1 \cdot p_2 = \epsilon_1 \epsilon_2 (1 - \cos \theta_{n-2})), \quad (4.3b)$$

$$\int \frac{-i d^n q (1, q_\mu)}{(2\pi)^n (-q^2 - 2kq + M^2)^\alpha} = \frac{\Gamma(\alpha - \frac{1}{2}n) (1, -k_\mu)}{(4\pi)^{n/2} \Gamma(\alpha) (M^2 + k^2)^{\alpha-n/2}}, \quad (4.4a)$$

Fig. 15 (c + d + f) = $-\text{Tr} O_A (\eta'(\rho_{(1)}^n) \theta(E_1 - E_2) \theta(E_1 - E_3) + (1 \leftrightarrow 2) + (1 \leftrightarrow 3))$.

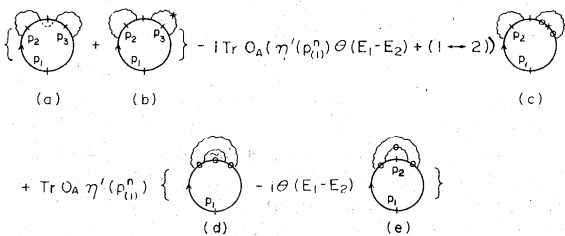


FIG. 21. Reduced form of diagrams in Fig. 15(c), 15(d), 15(f); [$p_{(j)} = -i(\mu - \epsilon_j)$, $j=1, 2, 3$]. Circles on propagators indicate that corresponding loops determine *bona fide* Feynman diagrams.

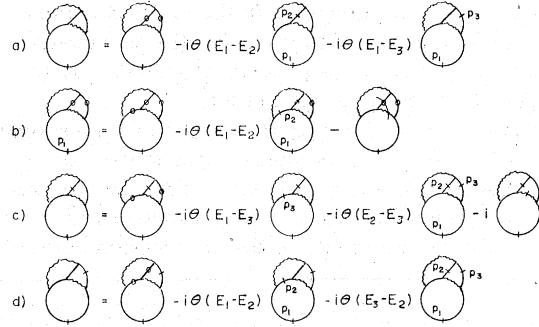


FIG. 22. Reduction of Fig. 15(g) to Feynman diagrams.

$$\int \frac{-i d^n q q_\mu q_\nu}{(2\pi)^n (-q^2 - 2kq + M^2)^\alpha} = \frac{\Gamma(\alpha - n/2)}{(4\pi)^{n/2} \Gamma(\alpha)} \frac{1}{(M^2 + k^2)^{\alpha-n/2}} \times [k_\mu k_\nu - g_{\mu\nu} (k^2 + M^2) / (\alpha - \frac{1}{2}n - 1)]. \quad (4.4b)$$

with the Minkowski metric being used in the last two equations.

Equation (4.1a) is finite as $m \rightarrow 0$ and $n \rightarrow 4$, and one easily derives

$$\Omega_{1a}^{(4)} = \lim_{m \rightarrow 0} D_F C_F^2 \alpha_s^2 \sum_a \left(-\frac{1}{8}\right) \left(\frac{\mu_a}{\pi}\right)^4, \quad (4.6)$$

where $\alpha_s \equiv g^2/4\pi$ defines the fine-structure constant.

For $m=0$, Eq. (4.1a) may also be evaluated easily using Eqs. (4.1b) (A8) in the Appendix. Notice that only the subtraction counterterm $\Sigma_1^{(2)}(-M^2)$ survives. Indeed, as $p^2 \rightarrow 0$ the self-energy $\Sigma_0^{(2)}(p) [= \Sigma_1^{(2)}(p^2)\not{p}]$ and its derivative vanishes as $(-p^2)^{n/2-2}$ and $(-p^2)^{n/2-3}$, respectively, provided $\text{Re}n > 6$.

This case is typical of dimensional regularization of infrared singularities. Therefore, the employed method may be stated in general terms. All calculations must be carried out in the region $\text{Re}n > n_0$, with a sufficiently large n_0 , where no

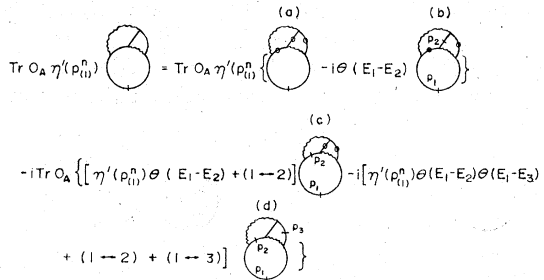


FIG. 23. Reduced form of Fig. 15(g). Circles on propagators indicate that corresponding loops determine Feynman diagrams [$p_{(i)}^2 = -i(\mu - \epsilon_i)$, $i=1, 2, 3$] as in Fig. 21.

$$\begin{aligned} \text{Tr } O_A \eta'(\rho_{(i)}^n) &= \text{Tr } O_A \eta'(\rho_{(i)}^n) \\ -i \text{Tr } O_A \left\{ \left[\eta'(\rho_{(i)}^n) \theta(E_1 - E_2) + (1 \leftrightarrow 2) \right] \right. \\ &\quad \left. - i \eta'(\rho_{(i)}^n) \theta(E_1 - E_2) \theta(E_1 - E_3) \right\} \end{aligned}$$

FIG. 24. Reduced form of Fig. 15(i). Circles on propagators indicate that corresponding loops determine *bona fide* Feynman diagrams. [$p_{(i)}^n = -i(\mu - \epsilon_i)$, $i = 1, 2, 3$].

infrared singularities are present. Then it will be legitimate to perform an analytic continuation of the resulting expressions from the region $\text{Re}n > n_0$ to the physical point $n = 4$ since the functions involved will be proven to be meromorphic in n .

It is important to know *a priori* that the physical quantity of interest is devoid of singularities, e.g., it is regular as $m \rightarrow 0$. Otherwise, the interchange of two limits $m \rightarrow 0$ and $n \rightarrow 4$ may not be justified and lead to an incorrect result even though possibly finite.

Returning to Eq. (4.1b) with the above remarks taken into consideration and applying the identity (3.13a), we find

$$\begin{aligned} \Omega_{1b}^{(4)} &= -D_F C_F^2 \alpha_s^2 \frac{\Gamma(\frac{1}{2}n - 1) \Gamma(3 - \frac{1}{2}n)}{(n - 4) 2^{n-1}} F_1(n, M) \\ &\quad \times \sum_a \left(\frac{M}{\mu_a} \right)^{n-4} \left(\frac{\mu_a}{\pi} \right)^4, \end{aligned} \quad (4.7)$$

where for later convenience the function $F_1(n, M)$ has been introduced:

$$F_1(n, M) = \frac{\sqrt{\pi} \Gamma^2(\frac{1}{2}n - 1)}{2\Gamma(n - 1/2) \Gamma^2(n - 2)} \left(\frac{M^2}{4\pi^3} \right)^{3n/2-6}. \quad (4.8)$$

In Eq. (4.1c) we first evaluate the loop integral using Feynman parameters. Performing the Wick rotation from the Euclidean to Minkowski momenta, $q^n \rightarrow -iq^n$, and using Eqs. (4.4) one derives

$$\begin{aligned} \text{Tr } O_A \eta'(\rho_{(i)}^n) &= \text{Tr } O_A \eta'(\rho_{(i)}^n) \left\{ \text{(a)} + i\theta(E_1 - E_2) \text{(b)} \right\} \\ &\quad + \text{Tr } O_A \eta'(\rho_{(i)}^n) \left\{ \text{(c)} - \text{(d)} \right\} \end{aligned}$$

FIG. 25. Reduced form of Fig. 15(h). Undashed blobs designate the zero-density gluon propagators $\mathcal{D}'_i(q)$.

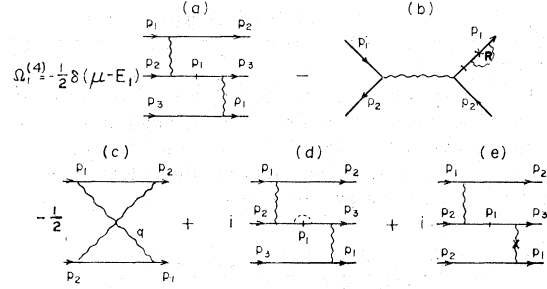


FIG. 26. Quark self-energy corrections in terms of Feynman diagrams. (a) Double scattering of a quark (1) on the top of the Fermi sea ($\epsilon_1 = \mu$) from quarks (2, 3) in the Fermi sea ($\epsilon_{2,3} < \mu$). (b) Exchange scattering of quarks with a renormalized (R) self-energy correction. (c) u -channel backward scattering. (d), (e) Residual diagrams: Indices of incoming and outgoing quarks with identical momenta p_a are assumed to be contracted with the projection operator $(\not{p}_a + m)/(\not{p}_a^n + i\epsilon_a)|_{p_a^n = i\epsilon_a} \equiv \not{p}_a$. In (b) the x stands for the γ_n vertex insertion in the Feynman self-energy and in (d), (e)

$$\frac{1}{\not{p}} = \frac{d}{d p^n} \left(\frac{\not{p} + m}{p^n + i\epsilon} \right) \Big|_{p^n = i\epsilon}, \quad \text{crossed line} = \frac{d}{d p^n} \left(\frac{1}{p^2} \right) g_{\mu\nu}$$

All momenta p_a should be integrated over the phase space $[d^{n-1} p_a / (2\pi)^{n-1}] \theta(\mu - \epsilon_a)$.

$$\begin{aligned} \Omega_{1c}^{(4)} &= D_F C_F^2 \alpha_s^2 \frac{2(n-2)^3 \Gamma(3 - \frac{1}{2}n) \Gamma^2(\frac{1}{2}n - 2)}{(4\pi)^{n/2-2} \Gamma(n-2)} \\ &\quad \times \sum_a \int \prod_{i=1}^2 \frac{d^{n-1} p_i}{(2\pi)^{n-1}} \frac{\theta(\mu_a - \epsilon_i)}{2\epsilon_i} (p_1 p_2)^{n/2-2}. \end{aligned} \quad (4.9)$$

The final integration over two-particle phase space is evaluated from Eq. (4.3b) with the result

$$\Omega_{1c}^{(4)} = D_F C_F^2 \alpha_s^2 \frac{(n-2)^2}{16(n-4)^4} \sum_a F_2(n, \mu_a) \left(\frac{\mu_a}{\pi} \right)^4 \quad (4.10)$$

where $F_2(n, M)$ is given in terms of the above function (4.8),

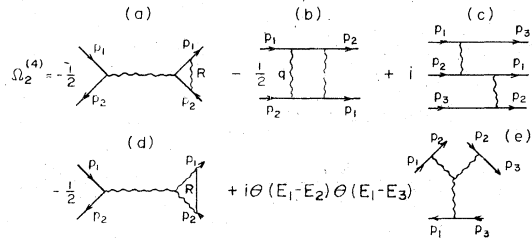


FIG. 27. Quark-gluon vertex corrections in terms of Feynman diagrams: (a), (d) Exchange scattering of quarks with a renormalized (R) vertex correction. (b) s -channel backward scattering. (c), (e) Scattering of three quarks. Rules are as in Fig. 26.

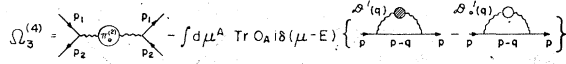


FIG. 28. (a) Exchange scattering with a second-order gluon self-energy correction $\pi_0^{(2)}$. (b) Medium polarization effects on the quark self-energy. The loop momentum q is Euclidean, whereas the external momentum p is Minkowski ($p^n = i\epsilon$).

$$F_2(n, M) = \frac{8(n-2)}{(3n-8)^2(n-3)} \frac{\Gamma^2(n-2)\Gamma(3-\frac{1}{2}n)}{\Gamma(\frac{3}{2}n-4)} \times F_1(n, M). \quad (4.11)$$

The three-particle phase-space integral in Eq. (4.1d) also can be done by means of Eq. (4.3b). One finds that $\Omega_{1d}^{(4)}$ vanishes identically

$$\Omega_{1d}^{(4)} = 0. \quad (4.12)$$

Finally, $\Omega_{1e}^{(4)}$ can be shown to be given by

$$\Omega_{1e}^{(4)} = D_F C_F^2 \alpha_s^2 \frac{-1}{4(n-3)(n-4)^2} \times \sum_a F_1(n, \mu_a) \left(\frac{\mu_a}{\pi}\right)^4, \quad (4.13)$$

which like Eq. (4.10) contains a second-order pole at $n=4$.

Now we combine Eqs. (4.7), (4.10), (4.13) and after some algebra discover that the residue of the second-order pole as well as that of the first-order one is identically zero. Although the algebra is slightly involved, simplification occurs by using logarithmic derivatives of relevant functions such as $\psi(z) = [\ln\Gamma(z)]'$ which satisfies the recursion relation $\psi(z+1) = \psi(z) + 1/z$. The final result of these calculations is

$$\Omega_{1(a+b+c+d+e)}^{(4)} = D_F C_F^2 \alpha_s^2 \times \sum_a \frac{1}{8} \left(\ln \frac{2\mu_a}{M} - \frac{9}{8} \right) \left(\frac{\mu_a}{\pi} \right)^4. \quad (4.14)$$

B. Quark-gluon vertex correction $\Omega_2^{(4)}$

Analytic expressions for the diagrams in Fig. 27 are as follows:

$$\Omega_{2(a+d)}^{(4)} = \frac{1}{2} g^2 \text{Tr} \int \prod_{a=1}^2 \frac{d^{n-1} p_a \theta(\mu - \epsilon_a)}{(2\pi)^{n-1}} \frac{1}{(p_1 - p_2)^2} \left[\frac{(\not{p}_1 + m) \gamma^\mu \lambda^i (\not{p}_2 + m) \Gamma_\mu^{(2) i} (p_1, p_2)}{2i\epsilon_1 2i\epsilon_2} \right], \quad (4.15a)$$

$$\Omega_{2b}^{(4)} = -\frac{1}{2} g^4 \text{Tr} \int \prod_{a=1}^2 \frac{d^{n-1} p_a \theta(\mu - \epsilon_a)}{(2\pi)^{n-1}} \int \frac{d^n q}{(2\pi)^n} \frac{1}{q^2 (p_1 - p_2 - q)^2} \left\{ \frac{\gamma_\nu \gamma^j (\not{p}_1 + m) \gamma^\mu \lambda^i (\not{p}_1 - \not{q} + m) \gamma^\nu \lambda^j (\not{p}_2 + m) \gamma_\mu \lambda^i (\not{p}_2 + \not{q} + m)}{2i\epsilon_1 [(p_1 - q)^2 - m^2] 2i\epsilon_2 [(p_2 + q)^2 - m^2]} \right\}, \quad (4.15b)$$

$$\Omega_{2c}^{(4)} = -g^4 i \text{Tr} \int \prod_{a=1}^3 \frac{d^{n-1} p_a \theta(\mu - \epsilon_a)}{(2\pi)^{n-1}} \frac{1}{(p_1 - p_3)^2 (p_2 - p_3)^2} \left\{ \frac{\gamma_\nu \lambda^j (\not{p}_1 + m) \gamma^\mu \lambda^i (\not{p}_3 + m) \gamma^\nu \lambda^j (\not{p}_2 + m) \gamma_\mu \lambda^i (\not{p}_1 - \not{p}_3 + \not{p}_2 + m)}{2i\epsilon_1 2i\epsilon_2 2i\epsilon_3 [(p_1 - p_3 + p_2)^2 - m^2]} \right\}, \quad (4.15c)$$

$$\Omega_{2e}^{(4)} = g^4 i \text{Tr} \int \prod_{a=1}^3 \frac{d^n p_a \theta(\mu - \epsilon_a)}{(2\pi)^{n-1}} (-iC_{iij}) \frac{(\not{p}_2 + m) \gamma^\alpha \lambda^i (\not{p}_3 + m) \gamma^\nu \lambda^j (\not{p}_1 + m) \gamma^\beta \lambda^j}{2i\epsilon_2 2i\epsilon_3 2i\epsilon_1} \times \theta(\epsilon_1 - \epsilon_2) \theta(\epsilon_1 - \epsilon_3) \frac{(2p_3 - p_1 - p_2)_\alpha g_{\beta j} + (2p_1 - p_2 - p_3)_\nu g_{\alpha\beta} + (2p_2 - p_1 - p_3)_\beta g_{\alpha\nu}}{(p_1 - p_2)^2 (p_2 - p_3)^2 (p_1 - p_3)^2}. \quad (4.15d)$$

The renormalized vertex $\Gamma_\mu^{(2) i}$ in Eq. (4.15a) is given by

$$\Gamma_\mu^{(2) i} = \Gamma_{(a)\mu}^i + \Gamma_{(d)\mu}^i, \quad \Gamma_{(a)\mu}^i = \left\{ -g^2 \int \frac{d^n q}{(2\pi)^n} \frac{\gamma^\nu \lambda^j (\not{p}_2 - \not{q} + m) \gamma_\mu \lambda^i (\not{p}_1 - \not{q} + m) \gamma_\nu \lambda^j}{q^2 [(p_2 - q)^2 - m^2] [(p_1 - q)^2 - m^2]} \right\} + \gamma_\mu \lambda^i \Gamma_{1(\phi)}^{(2)}(-M^2), \quad (4.16a)$$

$$\Gamma_{(d)\mu}^i = \left\{ g^2 \int \frac{d^n q}{(2\pi)^n} (iC_{iij}) \frac{[(2p_1 - p_2 - q)_\beta g_{\alpha\mu} - (p_2 + p_1 - 2q)_\mu g_{\alpha\beta} + (2p_2 - p_1 - 2q)_\alpha g_{\mu\beta}] \lambda^j \gamma^\beta (\not{q} + m) \gamma^\alpha \lambda^i}{(p_1 - q)^2 (p_2 - q)^2 (q^2 - m^2)} \right\} + \gamma_\mu \lambda^i \Gamma_{1(\phi)}^{(2)}(-M^2) \quad (4.16b)$$

with subtraction counterterms $\Gamma_{1(\psi)}^{(2)}$ and $\Gamma_{1(G)}^{(2)}$, being defined in the Appendix by Eq. (A1). The trace over color indices may be easily taken by the use of the following simple identities:

$$\text{Tr}(\lambda^i \lambda^j \lambda^i \lambda^j) = (C_F - \frac{1}{2}C_A)C_F D_F, \quad (4.17a)$$

$$iC_{ij} \text{Tr}(\lambda^i \lambda^j \lambda^i) = -\frac{1}{2}C_A C_F D_F, \quad (4.17b)$$

where C_A is the eigenvalue of the second Casimir operator in the regular (gluon) representation, i.e., $C_A \delta_{jk} = (T^j T^k)_{jk}$, $(T^j)_{jk} \equiv -iC_{ijk}$.

In the zero quark mass limit the evaluation of the above equations simplifies enormously. Let us start with Eq. (4.15a) for $\Omega_{2a}^{(4)}$. First, we carry out the q integration in Eq. (4.16a) using the Feynman's parametrization method and setting $p_a^2 = m^2 = 0$. Doing the integrations over the Feynman parameters and substituting the result into Eq. (4.15a), we obtain [cf. Eq. (A8)]

$$\Omega_{2a}^{(4)} = D_F C_F (C_F - \frac{1}{2}C_A) \alpha_s^2 8\pi(n-2)F(n, M) \sum_a \int \prod_{i=1}^2 \frac{d^{n-1}p_i \theta(\mu_a - \epsilon_i)}{(2\pi)^{n-1} 2\epsilon_i} \left\{ \left[2(n-3) + \frac{8}{n-4} \right] \left(\frac{2p_1 p_2}{M^2} \right)^{n/2-2} - (n-2) \right\}. \quad (4.18)$$

Here the second-order pole represents infrared and mass singularities. The last term in the curly brackets determines the contribution of the subtraction counterterm $\Gamma_{1(\psi)}^{(2)}$. The integration over two-particle phase space yields

$$\Omega_{2a}^{(4)} = -D_F C_F (C_F - \frac{1}{2}C_A) \alpha_s^2 \sum_a \left[\frac{F_2(n, \mu_a)}{2(n-4)^2} + \frac{1}{8} \ln \left(\frac{2\mu_a}{M} \right) - \frac{1}{16} \right] \left(\frac{\mu_a}{\pi} \right)^4, \quad (4.19)$$

with F_2 being given by Eqs. (4.8) and (4.11). The last two terms in square brackets have resulted from the combination of the first and third terms in the integrand of Eq. (4.18) in the limit $n \rightarrow 4$. Obviously, the result (4.19) depends on the subtraction procedure chosen in Eq. (2.32).

Applying above steps to $\Omega_{2d}^{(4)}$ one can derive

$$\Omega_{2d}^{(4)} = D_F C_F (-\frac{1}{2}C_A) \alpha_s^2 16\pi(n-2)F(n, M) \sum_a \int \prod_{i=1}^2 \frac{d^{n-1}p_i \theta(\mu_a - \epsilon_i)}{(2\pi)^{n-1} 2\epsilon_i} \left\{ \left(\frac{2p_1 p_2}{M^2} \right)^{n/2-2} + \frac{3}{2}(n-2) \right\}, \quad (4.20)$$

where the second term in the curly brackets is due to the subtraction counterterm $\Gamma_{1(G)}^{(2)}$. After doing the final integration and some simple algebra Eq. (4.20) becomes

$$\Omega_{2d}^{(4)} = D_F C_F (\frac{1}{2}C_A) \alpha_s^2 \sum_a \left[\frac{F_2(n, \mu_a)}{2(n-4)} - \frac{3}{8} \ln \left(\frac{2\mu_a}{M} \right) + \frac{9}{16} \right] \left(\frac{\mu_a}{\pi} \right)^4. \quad (4.21)$$

We turn to the correction (4.15b) arising from s-channel backward scattering. Performing the necessary trace algebra in the numerator of Eq. (4.15b), one may reduce $\Omega_{2b}^{(4)}$ to the form

$$\begin{aligned} \Omega_{2b}^{(4)} &= D_F C_F (C_F - \frac{1}{2}C_A) \alpha_s^2 16\pi^2(n-2) \\ &\times \sum_a \int \prod_{i=1}^2 \frac{d^{n-1}p_i \theta(\mu_a - \epsilon_i)}{(2\pi)^{n-1} 2\epsilon_i} \\ &\times \int \frac{d^n q}{(2\pi)^n} \frac{-(n-4)[(p_1 - q)^2 (p_2 + q)^2 - q^2 (p_1 - p_2 - q)^2] + 4p_1 p_2 [q^2 + (p_1 - p_2 - q)^2]}{(p_1 - q)^2 (p_2 + q)^2 (p_1 - p_2 - q)^2 q^2}. \end{aligned} \quad (4.22)$$

Now it is easy to carry out the q integration introducing no more than two independent Feynman parameters. Completing the remaining integrations one finds

$$\Omega_{2b}^{(4)} = D_F C_F (C_F - \frac{1}{2}C_A) \alpha_s^2 \frac{(n-3)}{2(n-4)^2} e^{i\pi n/2} \sum_a F_2(n, \mu_a) \left(\frac{\mu_a}{\pi} \right)^4, \quad (4.23)$$

where terms which vanish as $n \rightarrow 4$ have been dropped. The complex phase factor is a consequence of the absorptive part of the s-channel amplitude. However, by applying two-particle unitarity to Eq. (4.15b) one can see without any difficulty that contributions arising from absorptive parts of two- and three-particle scattering amplitudes

exactly cancel:

$$\text{Im}\Omega_{2b}^{(4)} + \text{Im}\Omega_{2c}^{(4)} = 0. \quad (4.24)$$

Therefore, it is sufficient to evaluate only the real part of $\Omega_{2a}^{(4)}$. The reduced form of the numerator of Eq. (4.15c) is obtained from that of Eq. (4.22) by substituting $q = p_1 - p_3$. Thus, dropping

terms which vanish as $n \rightarrow 4$ one gets

$$\begin{aligned} \text{Re}\Omega_{2c}^{(4)} = & D_F C_F (C_F - \frac{1}{2} C_A) \alpha_s^2 16\pi^2 \\ & \times \sum_a \{I_s(n, \mu_a) + I_r(n, \mu_a)\} \end{aligned} \quad (4.25)$$

with singular and regular parts being broken up

$$I_s(n, \mu_a) = -2(n-2) \int \prod_{i=1}^3 \frac{d^{n-1} p_i \theta(\mu_a - \epsilon_i)}{(2\pi)^{n-2} 2\epsilon_i} \frac{1}{p_1 p_3}, \quad (4.26a)$$

$$\begin{aligned} I_r(n, \mu_a) = & 2(n-2) p \int \prod_{i=1}^3 \frac{d^{n-1} p_i \theta(\mu_a - \epsilon_i)}{(2\pi)^{n-2} 2\epsilon_i} \\ & \times \frac{p_1 p_3 + p_2 p_3 + p_1 p_2}{p_1 p_3 + p_2 p_3 - p_1 p_2} \frac{1}{p_1 p_3}. \end{aligned} \quad (4.26b)$$

The integral I_r is regular at $n=4$ since its integrand is constructed to be antisymmetric with respect to the interchange of the momenta p_1 and p_2 as $p_3 - p_1$. Unfortunately, we have not been able to evaluate Eq. (4.26b) analytically. However, by quite accurate estimates we found

$$I_r(4, \mu_a) = \frac{1}{16\pi^2} \left(\frac{\mu_a}{\pi}\right)^4 \delta, \quad \delta \approx 0.69. \quad (4.27)$$

The singular integral I_s is evaluated from Eq. (4.3b). Substituting $I_{r,s}$ into Eq. (4.25) one arrives at

$$\begin{aligned} \text{Re}\Omega_{2c}^{(4)} = & -D_F C_F (C_F - \frac{1}{2} C_A) \alpha_s^2 \\ & \times \sum_a \left\{ \frac{F_1(n, \mu_a)}{2(n-3)(n-4)} - \delta \right\} \left(\frac{\mu_a}{\pi}\right)^4. \end{aligned} \quad (4.28)$$

One is left with the contribution $\Omega_{2e}^{(4)}$ given by Eq. (4.15e). It can be easily evaluated via Eqs. (4.3b), (4.17b).

$$\Omega_{2e}^{(4)} = -D_F C_F (\frac{1}{2} C_A) \alpha_s^2 \sum_a \frac{F_1(n, \mu_a)}{2(n-3)(n-4)} \left(\frac{\mu_a}{\pi}\right)^4. \quad (4.29)$$

Finally, we combine Eqs. (4.19), (4.23), (4.25) and Eqs. (4.20), (4.23) into two groups

$$\begin{aligned} \Omega_{2(a+b+c)}^{(4)} = & D_F C_F (C_F - \frac{1}{2} C_A) \alpha_s^2 \\ & \times \sum_a \frac{1}{8} \left(\ln \frac{2\mu_a}{M} + \frac{\pi^2}{2} + \frac{3}{2} - 8\delta \right) \left(\frac{\mu_a}{\pi}\right)^4, \end{aligned} \quad (4.30)$$

$$\begin{aligned} \Omega_{2(d+e)}^{(4)} = & -\frac{1}{2} D_F C_F C_A \alpha_s^2 \sum_a \frac{1}{8} \left(3 \ln \frac{2\mu_a}{M} - \frac{5}{2} \right) \\ & \times \left(\frac{\mu_a}{\pi}\right)^4. \end{aligned} \quad (4.31)$$

On the basis of remarks made at the end of the previous sub-section we find a complete cancellation of all poles at $n=4$.

C. Gluon self-energy correction Ω_3^4

The problem of gluon self-energy corrections is virtually identical to that of finding the correlation energy of the electron gas. The latter has a long history which dates back to original works of Bohm and Pines²⁵ and Gell-Mann and Brueckner.²⁶ In particular, the last two authors investigated the correlation energy of the nonrelativistic electron gas in the framework of quantum field theory. Subsequently, Fradkin²⁷ developed a general approach applicable to relativistic systems, as well, and Akhiezer and Peletminskii²⁸ carried out detailed calculations of the thermodynamic potential of the relativistic electron gas in $\alpha \ln \alpha$ approximation. Unfortunately, these authors failed to define in their theory a systematic renormalization procedure.

Here we will reproduce the result of Akhiezer and Peletminskii on the basis of our general approach which incorporates renormalization effects systematically (see Fig. 28).

A distinct feature of the problem is the existence of the plasmon eigenmode in the electron or quark systems which causes the breakdown of the ordinary perturbation theory. The breakdown appears in the form of "infrared" divergences (see below). It should be emphasized that these infrared divergences have qualitatively a different nature than those encountered throughout the preceding discussion. The former are induced by the medium and require nonvanishing fermion densities, whereas the latter are present *ab initio* due to the masslessness of the photon or gluon. The first type of divergences can be regulated by summing up certain class of diagrams which effectively makes the photon massive. Therefore, in general, the same mechanism can be used to regulate the standard infrared divergences as well. However, it is not necessary to do so if the system is known to be free of standard infrared divergences as a result of intrinsic cancellations. This cancellation is exactly what occurs in the case of the quark gas. As has been shown explicitly in preceding subsections, all infrared divergences of the standard type have cancelled out among themselves in the thermodynamic potential.

After these preliminary remarks we proceed to the analysis of $\Omega_3^{(4)}$ which is graphically represented in Fig. 28. It is given explicitly by

$$\Omega_{3a}^{(4)} = -\frac{1}{2} g^4 \text{Tr} \int \prod_{a=1}^2 \frac{d^{n-1} p_a \theta(\mu - \epsilon_a)}{(2\pi)^{n-1}} \left\{ \frac{\not{p}_1 + m}{2i\epsilon_1} \frac{\lambda^i \gamma^\mu \pi_{0\mu\nu}^{R(2)}(p_1 - p_2) \lambda^i \gamma^\nu}{(p_1 - p_2)^4} \frac{\not{p}_2 + m}{2i\epsilon_2} \right\}, \quad (4.32a)$$

$$\Omega_{3b}^{(4)} = g^2 \int \frac{d^n q}{(2\pi)^n} \text{Tr} \int d\mu^A O_A \int \frac{d^{n-1} p}{(2\pi)^{n-1}} i\delta(\mu - \epsilon) \frac{(\not{p} + m)}{2i\epsilon} \gamma^\mu \lambda^i \frac{(\not{p} - \not{q} + m) \gamma^\nu \lambda^j}{(p - q)^2 - m^2} \{ \mathfrak{D}_{\mu\nu}^{ij}(q) - \mathfrak{D}_{0\mu\nu}^{ij}(q) \}. \quad (4.32b)$$

Equation (4.32a) can be evaluated directly. By definition the renormalized polarization operator [cf. Eq. (2.49)]

$$\pi_{0\mu\nu}^{R(2)} = (g_{\mu\nu} q^2 - q_\mu q_\nu) \pi_0^{R(2)}(q^2) \quad (4.33)$$

with

$$\pi_0^{R(2)}(q^2) = \pi_0^{(2)}(q^2) - \pi_0^{(2)}(-M^2),$$

$\pi_0^{(2)}(q^2)$ being given in the Appendix by Eq. (A7).

Hence, the correction $\Omega_{3a}^{(4)}$ can be easily calculated for $\alpha = 1$ and $m = 0$ with the following result:

$$\Omega_{3a}^{(4)} \underset{m \rightarrow 0}{=} -\frac{1}{2} D_F C_F \left(\frac{5}{3} C_A - \frac{4}{3} N_F D_F C_F / D_A \right) \alpha_s^2 \times \sum_a \frac{1}{8} \left\{ \ln \left(\frac{2\mu_a}{M} \right) - 1 \right\}. \quad (4.34)$$

Equation (4.32b) requires careful treatment. As was indicated earlier the gluon propagator $\mathfrak{D}_{\mu\nu}(q)$ is not amenable to a simple perturbative expansion since higher-order terms of its perturbation series give rise to singularities at $q^2 = 0$. For this reason we separate in the polarization operator $\pi_{\mu\nu}$ the piece $\Delta_{\mu\nu}$ which is responsible for the breakdown of the perturbation theory. Evidently $\Delta_{\mu\nu}$ is completely determined by the contribution of the matter field,

$$\pi_{\mu\nu}^{R(2)} = \pi_{0\mu\nu}^{R(2)} + \Delta_{\mu\nu}. \quad (4.35a)$$

In the *zero-temperature* limit one has

$$\Delta_{\mu\nu}^{ij}(q) = \left(-g^2 \int \frac{d^n k}{(2\pi)^n} \text{Tr} \lambda^i \gamma_\mu S(k) \lambda^j \gamma_\nu S(k - q) \right) - (\mu = 0), \quad (4.35b)$$

where the term ($\mu = 0$) stands for the quark contribution to $\pi_{0\mu\nu}^{R(2)}$. Equation (4.35b) can be simplified by the reduction method of Sec. III. Repeating the steps leading to Eq. (3.6) from Eq. (3.5) one derives

$$\Delta_{\mu\nu}^{ij}(q) = -g^2 2 \text{Re} \left\{ \text{Tr} \int \frac{d^{n-1} k \theta(\mu - \epsilon_k)}{(2\pi)^{n-1}} \lambda^i \gamma_\mu \frac{(\not{k} + m)}{2\epsilon_k} \times \lambda^j \gamma_\nu \frac{(\not{k} - \not{q} + m)}{(k - q)^2 - m^2} \right\}_{k=i\epsilon_k}, \quad (4.36)$$

which can be shown to obey the transversality con-

dition $q^\mu \Delta_{\mu\nu}(q) = 0$. Hence, the decomposition similar to Eq. (2.45) is suggested:

$$\Delta_{\mu\nu}(q) = (g_{\mu\nu} q^2 - q_\mu q_\nu) \Delta_{\text{tr}}(q) + Q_\mu Q_\nu \Delta_2(q). \quad (4.37)$$

Further, we express the structure functions of the gluon propagator (2.45) in terms of π_0^R , Δ_{tr} , and Δ_2 . By means of the Dyson equation (2.48) one finds

$$\mathfrak{D}'_{\mu\nu}(q) = (g_{\mu\nu} q^2 - q_\mu q_\nu) \frac{1}{q^4} d_{\text{tr}}(q) + \alpha \frac{q_\mu q_\nu}{q^4} + \frac{Q_\mu Q_\nu}{q^4} d_2(q), \quad (4.38)$$

$$d_{\text{tr}} = (1 - \pi_0^R - \Delta_{\text{tr}})^{-1}, \quad (4.38a)$$

$$d_{\text{tr}} + d_2 = (1 - \pi_0^R - \Delta_{\text{tr}} - \Delta_2)^{-1}. \quad (4.38b)$$

Returning to Eq. (4.32b) we may rewrite it in the form [cf. Eq. (4.36)]

$$\Omega_{3b}^{(4)} \underset{1/\beta \rightarrow 0}{=} \int \frac{d^n q}{(2\pi)^n} \int d\mu^A \left\{ \frac{1}{2} \frac{d}{d\mu_A} \Delta_{\mu\nu}^{ij}(q) \right\} \times \{ \mathfrak{D}_{\mu\nu}^{ij}(q) - \mathfrak{D}_{0\mu\nu}^{ij}(q) \}, \quad (4.39)$$

which upon substitution of Eqs. (4.37), (4.38) simplifies to

$$\Omega_{3b}^{(4)} \underset{1/\beta \rightarrow 0}{=} \frac{1}{2} D_A \int \frac{d^n q}{(2\pi)^n} \{ 2[\ln(1 - \Delta_{\text{tr}} + \Delta_{\text{tr}})] + [\ln(1 - \Delta_{\text{tr}} - \Delta_2) + \Delta_{\text{tr}} + \Delta_2] \} \quad (4.40)$$

accurate to order g^4 . Equation (4.40) has been first derived by Akhiezer and Peletminskii²⁸ in QED in slightly different notation. To exhibit medium-induced infrared singularities referred to above, we write down integral representations of the structure functions Δ_{tr} and Δ_2 extracted from Eqs. (4.36), (4.37). Setting $m = 0$ in Eq. (4.36) we introduce spherical variables according to

$$\begin{aligned} q^4 &= Q \cos \varphi, \quad |\vec{q}| = Q \sin \varphi, \\ |\vec{k}| &= \epsilon_k \equiv \mu_a \sqrt{t}, \\ kq &= \mu_a Q \sqrt{t} (i \cos \varphi + \cos \theta \sin \varphi), \\ u &\equiv \cos \theta. \end{aligned} \quad (4.41)$$

Using the identity $\text{Tr}(\lambda^i \lambda^j) = D_F C_F / D_A \delta^{ij}$ one finds

$$\Delta_{\text{tr}} + \Delta_2 = - (D_F C_F / D_A) \alpha_s \sum_a \frac{4}{\pi} \frac{\mu_a^4}{Q^2} \int_0^1 t dt \int_{-1}^1 \frac{(1-u^2) du}{Q^2 - 4\mu_a^2 t \sin^2 \varphi (u + i \cot \varphi)^2}, \quad (4.42a)$$

$$3\Delta_{\text{tr}} + \Delta_2 = (D_F C_F / D_A) \alpha_s \sum_a \frac{8}{\pi} \frac{\mu_a^4}{Q^2} \int_0^1 t dt \int_{-1}^1 \frac{(u + i \cot \varphi)^2 du \sin^2 \varphi}{Q^2 - 4\mu_a^2 t \sin^2 \varphi (u + i \cot \varphi)^2}. \quad (4.42b)$$

We see that as $Q^2 \rightarrow 0$, $\Delta_{\text{tr},2} \sim \mu^2/Q^2$ and the perturbative expansion of the integrand in Eq. (4.40) gives rise to the medium-induced ($\mu_\beta = 0$) infrared divergences.

Akhiezer and Peletminskii²⁸ evaluated Eq. (4.40) given Eqs. (4.42) in the leading logarithm approximation $\alpha_s \ln \alpha_s$. Recently, Freedman and McLerran^{16b,16c} have further calculated terms of order α_s^2 . The final result of these calculations is

$$\Omega_{3b}^{(4)} = D_A \bar{\alpha}_s^2 \sum_{a,b} \frac{1}{8} \left(\frac{\mu_a}{\pi} \right)^2 \left(\frac{\mu_b}{\pi} \right)^2 \times \left[\ln \frac{\bar{\alpha}_s}{\pi} \sum_c \frac{\mu_c^2}{\mu_a^2} + \phi \left(\frac{\mu_a^2}{\mu_b^2} \right) - 0.93 \right], \quad (4.43)$$

where $\bar{\alpha}_s \equiv (D_F C_F / D_A) \alpha_s$ and the function $\phi(x)$ is given by

$$\phi(x) = \frac{1}{6} \left(\sqrt{x} - \frac{1}{\sqrt{x}} \right)^4 \ln |1-x| + \frac{4}{3} \left(\sqrt{x} + \frac{1}{\sqrt{x}} \right) \ln(1+\sqrt{x}) - \left(1 + \frac{1}{6}x \right) \ln x. \quad (4.44)$$

$$\Omega_{m \rightarrow 0, 1/\beta \rightarrow 0}^{(4)} = D_F C_F \beta^{(2)}(\alpha_s) \sum_a \ln \left(\frac{2\mu_a}{eM} \right) \left(\frac{\mu_a}{2\pi} \right)^4 - D_F C_F \alpha_s^2 \sum_a \left\{ \frac{5}{8} C_A + \left(C_F - \frac{1}{2} C_A \right) \left(\pi^2 + \frac{21}{4} - 16\delta \right) \right\} \left(\frac{\mu_a}{\pi} \right)^4 + (D_F^2 C_F^2 / D_A) \alpha_s^2 \sum_{a,b} \left\{ 2 \ln \left(\sum_c \frac{\mu_c^2}{\mu_a^2} \frac{D_F C_F}{D_A} \frac{\alpha_s}{\pi} \right) + 2\phi \left(\frac{\mu_a^2}{\mu_b^2} \right) - 1.86 \right\} \left(\frac{\mu_a \mu_b}{4\pi^2} \right)^2, \quad (4.46c)$$

with

$$\phi_{(0)}(x) = (1-x)^{1/2} \left(1 - \frac{5}{2}x \right) + \frac{3}{2}x^2 \ln \left[\frac{1+(1-x)^{1/2}}{x^{1/2}} \right], \quad (4.47a)$$

$$\phi_{(2)}(x) = 3 \left\{ (1-x)^{1/2} - x \ln \left[\frac{1+(1-x)^{1/2}}{x^{1/2}} \right] \right\} - 2(1-x)^2, \quad (4.47b)$$

$$\beta^{(2)}(\alpha_s) = \left\{ -\frac{11}{3} C_A + \frac{4}{3} N_F D_F C_F / D_A \right\} \alpha_s^2. \quad (4.48)$$

In Eq. (4.46c) $\delta = 0.7$ by Eq. (4.27) and $\phi(x)$ is given by Eq. (4.44). One easily recognizes $\beta^{(2)}(\alpha_s)$ as

Equations (4.34) and (4.43) taken together determine a fourth-order correction to the thermodynamic potential generated by the vacuum and medium polarization effects.

D. Summary of results and discussion

Now we can combine the previous results to find the thermodynamic potential of the massless quark gas in the ground state

$$\Omega \equiv \Omega^{(0)} + \Omega^{(2)} + \Omega^{(4)} + O(\alpha_s^3 \ln \alpha_s), \quad (4.45)$$

where $\Omega^{(0,2)}$ and $\Omega^{(4)}$ in the Feynman gauge are inferred from Eqs. (3.6'), (3.18) and Eqs. (4.14), (4.30), (4.31), (4.34), (4.43) respectively,

$$\Omega_{1/\beta \rightarrow 0}^{(0)} = D_F \sum_a \left(-\frac{4}{3} \pi^2 \right) \phi_{(0)} \left(\frac{m_a^2}{\mu_a^2} \right) \left(\frac{\mu_a}{2\pi} \right)^4, \quad (4.46a)$$

$$\Omega_{1/\beta \rightarrow 0}^{(2)} = D_F C_F \alpha_s \sum_a (2\pi) \phi_{(2)} \left(\frac{m_a^2}{\mu_a^2} \right) \left(\frac{\mu_a}{2\pi} \right)^4, \quad (4.46b)$$

the Gell-Mann-Low function in the lowest nontrivial order. It is known to determine the rate of change of the effective charge $\alpha_s(M)$ as a function of the subtraction point M

$$M \frac{d\alpha_s(M)}{dM} = \frac{1}{2\pi} \beta(\alpha_s(M)). \quad (4.49)$$

Recalling that $\mu_a = (\mu_A O^A)_{aa}$ one directly infers from Eqs. (4.45)–(4.48) fermion densities, conjugate to μ_A [cf. Eq. (2.1)].

$$N_A = - \frac{\partial \Omega}{\partial \mu_A}. \quad (4.50)$$

Now the effect of various definitions of the renormalized coupling $\alpha_s(M)$ will be discussed. Recall that $\alpha_s(M)$ has been defined by Eqs. (2.4c), (2.23a), (2.32), (2.47) and by equations given in the Appendix. The latter depend on the gauge fixing parameter which determines a gauge dependence of the renormalized coupling. In particular, it is easy to find the relationship between the $\alpha_F(M)$ and $\alpha_L(M)$ couplings appropriate to the Feynman ($\alpha=1$) and to the Landau ($\alpha=0$) gauges, respectively.

$$\alpha_F(M) = \alpha_L(M) + \left(\frac{5}{16\pi} C_A \right) \alpha_L^2(M) + O(\alpha_L^3). \quad (4.51)$$

Evidently, the thermodynamic potential is a gauge-invariant quantity, which is apparent from Eq. (3.1) since it is given in terms of bare densities. However, the parametrization of Ω in terms of the gauge-dependent coupling $\alpha_s(M, \alpha)$ introduces, through renormalization counterterms, an implicit α dependence in the analytic form of Eq. (4.46c). We would like to reiterate that the thermodynamic potential is independent of the value of α .

There exists an alternative subtraction procedure which defines α_s independent of α . Indeed following 't Hooft²² we require renormalization constants $Z_i^{(2)}$, $i=1, 2, 3$, to be given by pure pole terms $\sim 1/(n-4)$ of Eqs. (A1)-(A3) obtained from the Taylor-series expansion of Eqs. (A4)-(A7) at $n=4$; In general, one would choose all coefficients $\{a_{mk}(i), k=0\}$ in Eq. (2.7) to be zero. It is easy to verify explicitly in second order that the resulting coupling $\alpha_H(M)$ is independent of α . In general, it is known that the above definition of the renormalization constants leads to the α -independent Gell-Mann-Low function $\beta(\alpha_H)$.²⁹ For later reference we give the relationship between the two couplings $\alpha_{L,H}(M)$ introduced above

$$\alpha_L = \alpha_H - \frac{1}{4\pi} \beta^{(2)}(\alpha_H)(2 + \ln 4\pi + C) - \frac{1}{4\pi} \alpha_H^2 \left(\frac{113}{36} C_A - \frac{4}{9} N_F D_F C_F / D_A \right), \quad (4.52)$$

where $C=0.577$ is Euler's number.

Evidently a perturbative expansion of physical quantities as a power series in $\alpha_H(M)$ would be rather awkward due to the appearance of irrational numbers $\ln 4\pi$ and C .

Finally, we will discuss the optimal choice of the subtraction point M . The truncated perturbation series (4.45) for $\Omega(\mu, m(M), \alpha_s(M), M)$ is independent of M within terms of higher order than those present, which may be directly checked

via the Gell-Mann-Low equation (4.49). In all orders this independence is clearly seen from Eq. (3.2) which is given by the bare Green's function. One would naturally choose M such as to minimize the relative contribution of higher-order terms or, more precisely, to suppress potentially large logarithmic factors $[\ln(\mu_a/M)]^n$ systematically appearing in higher orders. Thus, one arrives at the optimal choice

$$M \sim \mu_a. \quad (4.53)$$

An important remark should be made. At high fermion densities such that $\mu_a \gg m_a$ for some "a" the condition (4.53) assumes the absence of terms $\ln(m_a/M)$ in the perturbation series. This requirement is met due to the absence of mass singularities. Of course terms of the type $(m/M) \ln(m/M)$ would not invalidate the perturbation expansion.

V. THERMODYNAMICS OF THE QUARK GAS

The equation of state for the quark gas will now be analyzed. Tentative neutron-matter densities, at which a transition to the quark phase can occur, will be found. Equations of state of various neutron-matter models will be used in this analysis.³⁰

A. Neutron-quark transition densities

The case of physical interest has colored gauge group $SU(N)$ with $N=3$ and flavor group $SU(N_F)$ with $N_F=2, 3$. The Casimir eigenvalues appearing in Eqs. (4.46), (4.47) are

$$2NC_F = D_A = N^2 - 1, \quad C_A = D_F = N \quad (5.1)$$

where quarks are assumed to be in the fundamental representation.

Now the conserved flavor charges \hat{O}_A and their conjugate chemical potentials μ^A will be specified. Actually there is only one independent chemical potential μ_B , which corresponds to the baryon number $B \equiv \frac{1}{3} N_B$ conservation (the factor of $\frac{1}{3}$ was introduced purely for convenience). The remaining chemical potentials $\mu_{A \neq B}$ are fixed by various conditions. Indeed, the chemical potential μ_Q conjugate to the electric charge is determined from the electric neutrality condition

$$Q \equiv \frac{1}{3} N_Q = - \frac{1}{3} \frac{\delta \Omega}{\delta \mu_Q} = 0. \quad (5.2)$$

Here again the factor of $\frac{1}{3}$ is for convenience. The chemical potential μ_s conjugate to the strangeness S is fixed by the requirement that the energy E of the system in thermodynamic equilibrium should have a minimum with respect to variations of the strangeness $S \equiv N_s$,

$$\frac{\delta E}{\delta S} = \mu_S = 0, \quad (5.3a)$$

$$E = \Omega + \mu^A N_A. \quad (5.3b)$$

In general, a similar condition applies also to the charm $C \equiv N_C$ thereby implying $\mu_C = 0$. However, the charm quarks will not be entertained here, since the chemical potentials of interest are $\mu_B \lesssim 1$ GeV which exclude the existence of heavy quarks, i.e., with mass $m_C \gtrsim 1.5$ GeV.

Furthermore, the excitation of charmed degrees has a negligible effect in the gluon polarization operator.

The contribution of the charged leptons to the thermodynamic potential can also be ignored since the relevant chemical potential μ_Q is small ($\mu_Q/\mu_B \ll 1$ (see below)). At this point it is helpful to notice that the φ , \mathcal{N} , and λ quark numbers are coupled to the following combinations of the chemical potentials considered above:

$$\mu_\varphi = \mu_B + 2\mu_Q, \quad (5.4a)$$

$$\mu_{\mathcal{N}} = \mu_\lambda = \mu_B - \mu_Q, \quad (5.4b)$$

which may be easily inferred from the identity

$$\mu^A \hat{O}_A = 3(\mu_B \hat{B} + \mu_Q \hat{Q}). \quad (5.5)$$

Obviously, the μ_a , $a=1, \dots, N_F$ in Eqs. (4.56) coincide with chemical potentials introduced in Eqs. (5.4), i.e.,

$$\mu_1 = \mu_\varphi, \quad \mu_2 = \mu_{\mathcal{N}}, \quad \mu_3 = \mu_\lambda. \quad (5.6)$$

We proceed to the discussion of the equation of state of the quark gas. To begin with, quark masses will be completely ignored. The $m \neq 0$ effects will be discussed later.

The relation between the thermodynamic potential Ω and the pressure P is known to be

$$\Omega = -PV. \quad (5.7)$$

Recall that in the previous sections the volume V has been suppressed. From Eqs. (4.45), (4.46) and Eq. (5.1) with $N=3$ we immediately infer the equation of state for two, $P^{(2)}$ ($N_F=2$), and three, $P^{(3)}$ ($N_F=3$), flavor massless quark gas

$$P^{(2)} = \frac{1}{4\pi^2} \mu_B^4 \left\{ (a^4 + b^4) \left[1 - 2 \left(\frac{\alpha_F}{\pi} \right) \right] - a^2 b^2 \left[\ln \left(\frac{c^2}{a^2 b^2} \right) + \phi \left(\frac{a^2}{b^2} \right) + \phi \left(\frac{b^2}{a^2} \right) - 1.36 \right] \left(\frac{\alpha_F}{\pi} \right)^2 \right. \\ \left. + \left[a^4 \left(\frac{32}{3} \ln a - \ln c \right) + (a-b) \right] \left(\frac{\alpha_F}{\pi} \right)^2 - \left[\ln \left(\frac{\alpha_F}{\pi} \right) - 0.25 \right] (a^2 + b^2)^2 \left(\frac{\alpha_F}{\pi} \right)^2 \right\}, \quad (5.8a)$$

$$P^{(3)} = \frac{1}{4\pi^2} \mu_B^4 \left\{ (a^4 + 2b^4) \left[1 - 2 \left(\frac{\alpha_F}{\pi} \right) \right] + 2a^2 b^2 \left[\ln(ab) - \phi \left(\frac{a^2}{b^2} \right) - \phi \left(\frac{b^2}{a^2} \right) + 3.7 \right] \left(\frac{\alpha_F}{\pi} \right)^2 \right. \\ \left. + \left[a^4(10 \ln a + 1.17) + 2b^4(11 \ln b + 1.17) \right] \left(\frac{\alpha_F}{\pi} \right)^2 - \left[\ln \frac{3\alpha_F}{2\pi} + 0.92 \right] (a^2 + 2b^2)^2 \left(\frac{\alpha_F}{\pi} \right)^2 \right\}, \quad (5.8b)$$

where the subtraction point M was chosen to be [cf. Eqs. (4.46c), (4.53)]

$$M = \frac{2}{e} \mu_B. \quad (5.9)$$

The function $\phi(x)$ was defined in Eq. (4.44) and

$$a = 1 + 2\mu_Q/\mu_B, \quad b = 1 - \mu_Q/\mu_B, \quad c = 1 + \mu_Q/\mu_B. \quad (5.10)$$

Quark densities may be inferred from Eq. (5.8):

$$n_B^{(i)} = \frac{dP^{(i)}}{d\mu_B}, \quad i=2, 3, \quad (5.11a)$$

$$n_Q^{(i)} = \frac{dP^{(i)}}{d\mu_B}, \quad i=2, 3, \quad (5.11b)$$

with the electroneutrality condition (5.2) being imposed.

To analyze Eqs. (5.8), (5.11) one needs to know the running charge $\alpha_F = \alpha_F(2/e)\mu$. The Gell-Mann-Low equation (4.49) relates values of $\alpha_F(M)$ at various points. Notice that $\beta(\alpha_H)$ in (4.49) has been computed up to terms of order α_H^3

$$\beta(\alpha_H) = \beta^{(2)} \alpha_H^2 + \beta^{(3)} \alpha_H^3 \quad (5.12)$$

with $\beta^{(2)}$ given by Eq. (5.58) and $\beta^{(3)}$ by³¹

$$4\pi \beta^{(3)} = -\frac{34}{3} C_A^2 + \left(\frac{20}{3} C_A + 4C_F\right) C_F N_F D_F / D_A. \quad (5.13)$$

Thus, one can parametrize $\alpha_H(M)$ and via Eqs. (4.51), (4.52) also $\alpha_{F,L}(M)$ in terms of $\alpha_H(M_0)$ or $\alpha_{F,L}(M_0)$, where M_0 is a conveniently chosen point. The resulting curves for various values of $\alpha_L(M_0)$ with $M_0=3$ GeV are shown in Fig. 29. For the same initial value of $\alpha_L(3$ GeV) the effective charge of two-flavor gas turns out to be slightly larger than that of three-flavor gas.

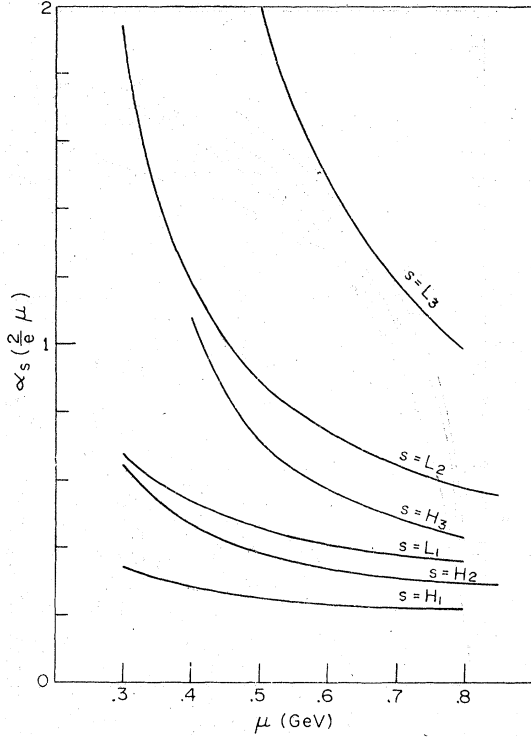


FIG. 29. Behavior of the effective charge $\alpha_H(2/e)\mu$ according to Eqs. (4.42), (4.48), (5.1), (5.12), (5.13) with $N=N_F=3$. Various reference values are considered $\alpha_{H_{1,2,3}}(3 \text{ GeV}) = 0.14, 0.17, 0.20$. The curves $\alpha_L(M)$ are obtained from those of $\alpha_H(M)$ by Eq. (4.52): $\alpha_{L_{1,2,3}}(3 \text{ GeV}) = 0.20, 0.26, 0.32$.

Notice that the values of $\alpha_{L_i}(M)$ are at least as much as twice larger than those of $\alpha_{H_i}(M)$. Clearly, the distinction between two effective charges $\alpha_H(M)$ and $\alpha_L(M)$ arises beyond the Born

approximation. However, the contributions of the Born terms in Ω corresponding to various choices of the expansion parameter $\alpha_s(M)$, $s=L, H, F$ may differ significantly for a given value $\alpha_s(M_0) = \alpha_0$. Our preferred choice is $\alpha_L(M)$ for two reasons.

Firstly, in the Landau gauge unrenormalized (α_0) as well as renormalized (α) gauge parameters are identically zero. Therefore, an additional functional dependence on the chemical potential μ through the running gauge parameter $\alpha(\mu)$ does not arise in higher orders of perturbation expansion.

Secondly, the ratios $(\Omega_H^{(4)}/\Omega_H^{(2)})$ and $(\Omega_L^{(4)}/\Omega_L^{(2)})$ inferred from Eq. (5.8) relate as two to one for the values of $\alpha_{L,H}$ considered in Fig. 29. Thus, the α_L appears to be more suitable expansion parameter for Ω than α_F or α_H .

Unfortunately, at present there is no consensus on the value of $\alpha_s(3 \text{ GeV})$. The values used above $\alpha_L(3 \text{ GeV}) \approx 0.3$ should be considered as a tentative choice being suggested by the phenomenological analyses of the existing experimental data on the deep-inelastic structure functions and electron-positron-annihilation cross section.³²

The chemical potential μ_Q has been numerically determined from Eq. (11b) for the values of μ_B of interest. It should be noted that the desired solution $\mu_Q = \mu_Q^{(i)}(\mu_B)$, $i=2, 3$, should correspond to the local minimum of the thermodynamic potential, i.e.,

$$\partial^2 \Omega / \partial \mu_Q^2 |_{\mu_Q = \mu_Q^{(i)}(\mu_B)} > 0.$$

By a direct numerical analysis it was found that $\mu_Q^{(2)} \approx -0.03 \mu_B$ and $\mu_Q^{(3)} = 0$. Since effects due to $\mu_Q^{(2)}$ are negligible, one may set effectively $\mu_Q^{(i)} = 0$, simplifying Eqs. (5.8), (5.11) to

$$P^{(2)}(\mu_B) = \mu_B^4 \left(\frac{1}{2\pi^2} \right) \left\{ 1 - 2 \left(\frac{\alpha_L}{\pi} \right) - \left[2.55 + 2 \ln \left(\frac{\alpha_L}{\pi} \right) \right] \left(\frac{\alpha_L}{\pi} \right)^2 \right\}, \quad (5.14a)$$

$$n^{(2)}(\mu_B) = \mu_B^3 \left(\frac{2}{\pi^2} \right) \left\{ 1 - 2 \left(\frac{\alpha_L}{\pi} \right) - \left[0.13 + 2 \ln \left(\frac{\alpha_L}{\pi} \right) \right] \left(\frac{\alpha_L}{\pi} \right)^2 \right\}, \quad (5.14b)$$

$$P^{(3)}(\mu_B) = \mu_B^4 \left(\frac{3}{4\pi^2} \right) \left\{ 1 - 2 \left(\frac{\alpha_L}{\pi} \right) - \left[4.69 + 3 \ln \left(\frac{\alpha_L}{\pi} \right) \right] \left(\frac{\alpha_L}{\pi} \right)^2 \right\}, \quad (5.15a)$$

$$n^{(3)}(\mu_B) = \mu_B^3 \left(\frac{3}{\pi^2} \right) \left\{ 1 - 2 \left(\frac{\alpha_L}{\pi} \right) - \left[2.44 + 3 \ln \left(\frac{\alpha_L}{\pi} \right) \right] \left(\frac{\alpha_L}{\pi} \right)^2 \right\}. \quad (5.15b)$$

Here the coupling $\alpha_L = \alpha_L(2/e)\mu_B$ has been introduced according to Eq. (4.51).

The functions (5.14a) and (5.15a) are plotted in Fig. 30 for various interaction strengths $\alpha_L(3 \text{ GeV}) = 0.2(L_1), 0.26(L_2), 0.32(L_3)$. They have to be compared with the equations of state for different

neutron-matter models presented in Fig. 30 by the curves $R-P$, $B-J$, $P-S$, and W . These models are due to Reide and Pandharipande,³³ Bethe and Johnson,³⁴ Pandharipande and Smith,³⁵ and Walecka.³⁶ The cross point P vs μ_B curves corresponding to the neutron matter and the quark

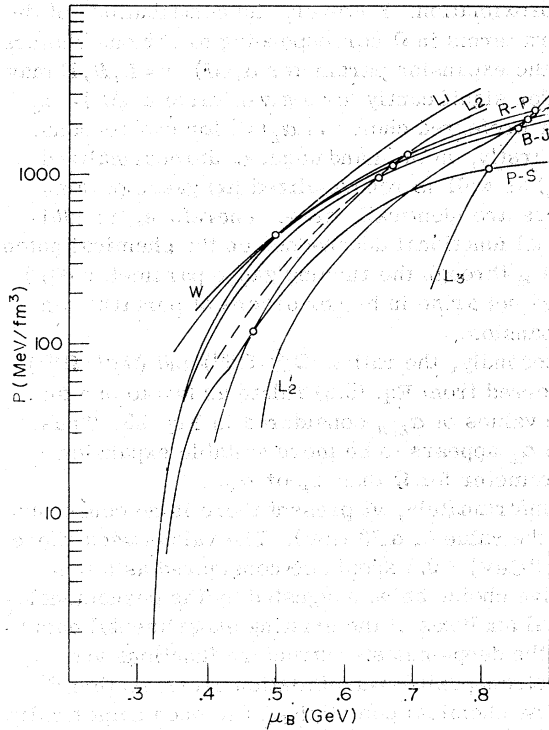


FIG. 30. L_2, L_3 are equations of state of the quark gas for effective charges α_{L_2, L_3} (see Fig. 29). The curve L_2' is the $N_F=2$ counterpart of L_2 . The dashed curve is obtained from L_2 after ignoring $\alpha_L^2(\ln\alpha_L)$ terms. $R-P, B-J, W, P-S$ represent equations of state in various neutron-matter models (see text).

gas determines the parameters of a phase transition between these two states of matter. This rule follows from the condition of thermodynamic equilibrium between two different phases (see, e.g., Chap. 8 of Ref. 37).

Comparison of Figs. 30 and 31 shows that the neutron-matter transition densities vary, in a broad range below $n_B=2$ baryons/ fm^3 , with the interaction-coupling $0.2 \leq \alpha_L(3 \text{ GeV}) \leq 0.32$. Unfortunately, the lower bound of the transition densities cannot be identified reliably as it is sensitive to the detailed behavior of the equations of state in the threshold region $\mu_B \geq 0.3 \text{ GeV}$. In this region the equation of state of the quark gas may be strongly affected by quark mass effects as well as the nonperturbative effects discussed in the following subsection. However, it should be noted that naive considerations do not rule out transition densities which are of order of the nuclear-matter densities ($n_B \approx 0.16$ baryons/ fm^3). For example, Eq. (5.15a) with $\alpha_L(3 \text{ GeV})=0.24$ determines an equation of state almost identical with the curve $B-J$ in Fig. 30, and is also represented in Fig. 31 by the dashed curve L .

The contribution of $\alpha_L^2(\ln\alpha_L)$ terms is exhibited

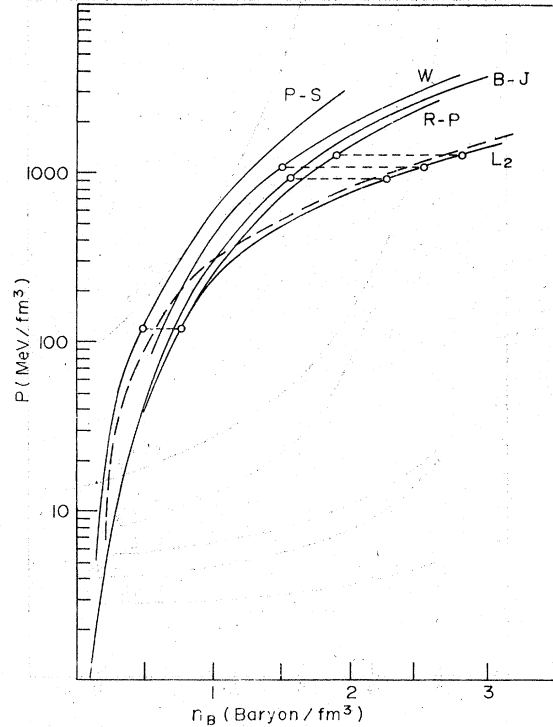


FIG. 31. The baryon number density n_B vs the pressure P in various neutron-matter models and the quark gas (see Fig. 30). Open circles indicate neutron-quark matter transition densities corresponding to the curves L_2 in Fig. 30. The dashed curve represents the equation of state of the quark gas for $\alpha_L(3 \text{ GeV})=0.24$.

in Fig. 30 by the deviation of the dashed curve from the curve L_2 . Although higher-order terms turn out to be negligible at high transition density, it is important to realize that they have an implicit effect on transition densities by determining the optimal choice of the subtraction point (5.9) and the coupling α_L .

The dependence on the number of flavors may be recognized by comparing, in Fig. 30, L_2' and L_2 which respectively represent equations of state for two- and three-flavor quark gas with the same interaction strength $\alpha_L(3 \text{ GeV})=0.26$. Evidently the neutron matter prefers transition to a three- rather than two-flavor quark phase since the former has a larger phase space.

One can see from Figs. 31 and 32 that after passing to the quark phase, matter becomes almost twice as dense, with the per baryon energy, ϵ , correspondingly larger. The increase in ϵ is given by $\Delta\epsilon = P\Delta(1/n_B) \sim 2 \text{ GeV}$ for $\alpha_L(3 \text{ GeV})=0.26$.

The presented analysis suggests that the neutron-quark phase transition may take place at neutron-matter densities $n_B < 2$ baryon/ fm^3 , provided $0.2 < \alpha_L(3 \text{ GeV}) < 0.3$; at the high end of the density

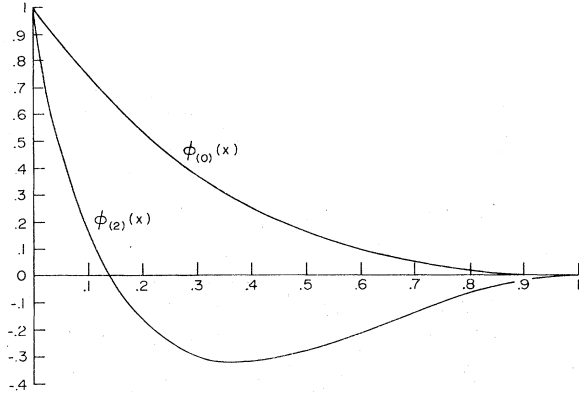


FIG. 32. The $\phi_{(0,2)}(x)$ are threshold factors of Eqs. (4.46).

range transition is a highly endoenergetic process.

The conclusion essentially remains unaffected if one uses the simple parametrization $\alpha_L(\mu) = 2\pi / (9 \ln \mu / \Lambda)$ with $0.2 < \alpha_L(3 \text{ GeV}) < 0.3$ or $100 \text{ MeV} < \Lambda < 300 \text{ MeV}$. This expression for the effective coupling $\alpha_L(\mu)$ is the solution of the Gell-Mann-Low equation (4.49) with $\beta(\alpha_L) = \beta^{(2)}(\alpha_L) = -9\alpha_L^2$ [see Eq. (4.48)]. Obviously, the larger the interaction strength $\alpha_L(3 \text{ GeV})$, the higher transition densities are. Note that for sufficiently small $\alpha_L(3 \text{ GeV})$ the transition may be entirely impossible.

It is important to emphasize that $\alpha_L(3 \text{ GeV})$ may be directly inferred from the phenomenology of QCD.

B. Discussion

The above conclusions should be considered in the light of the following remarks:

1. Tests for neutron-matter models are lacking. In particular, their reliability, at densities much higher than nuclear-matter densities ~ 0.16 baryon/ fm^3 , has been often questioned.³⁰ Notice, however, that three of the four models considered in Figs. 30, 31 predict rather close transition densities < 2 baryon/ fm^3 , supporting the model independence of our conclusions.

The model $P-S$ is distinct from the remaining ones in that it assumes a solid phase of neutron matter for $n_B > 0.35$ baryon/ fm^3 . Therefore, it is not surprising that it predicts much lower neutron-quark transition densities (see Fig. 31).

2. Perturbation theory is expected to break down in the transition region where confining forces become important. These forces are known to be responsible for the formation of neutrons from quarks and have been ignored in our analysis altogether. Therefore, the positions of transition points in Figs. 30 and 31 should not be taken too literally. However, they are expected to determine transition densities

approximately.

At sufficiently high densities, the quark gas develops the Debye screening of color which seems to provide a suppression mechanism for long-range confining forces. Indeed, if the confining forces are assumed to be effective at distances larger than d_c , the above mechanism becomes operative provided

$$d_c \geq 2r_D. \quad (5.16)$$

The Debye radius, r_D , is easily inferred from Eqs. (4.42a)

$$r_D^{-2} = Q^2 \Delta_2(Q) \\ = \frac{6\alpha_L((2/e)\mu_B)}{\pi} \mu_B^2. \quad (5.17)$$

Turning to Fig. 30, one finds that the condition (5.16) is met for the transition points indicated ($\mu_B > 0.4 \text{ GeV}$) if $d_c \sim 1 \text{ fm}$, given by the size of the neutron.

3. Quark mass effects remain to be discussed. The quark masses $\{m_a\}$ are known to be a measure of the chiral-symmetry breaking. In general, they consist of two components $m = m_D + m_B$. The first component m_D is generated *dynamically* and arises from the nonvanishing vacuum expectation of the mass operator $\bar{\psi}\psi$. The second component, m_B , is due to the *bare* mass present in the fundamental Lagrangian (2.3).

We will adopt the point of view that the spontaneously broken nature of the chiral symmetry is responsible to confining forces, which in the quark phases was suggested to be set off by the color screening. Correspondingly, in accord with pure perturbative approach of preceding sections, we will assume that $m_D = 0$ and $m = m_B$.

Let us return to the thermodynamic potential (4.45) and set $\mu_a = \mu_B$, $a = 1, \dots, N_F$ ignoring the neutrality condition (5.2) [cf. Eqs. (5.4) and (5.6)]:

$$P(\mu_B) = \frac{1}{4\pi^2} \mu_B^4 \sum_a \left\{ \phi_{(0)}\left(\frac{m_a^2}{\mu_B^2}\right) - \phi_{(2)}\left(\frac{m_a^2}{\mu_B^2}\right) \left(\frac{2\alpha_L}{\pi}\right) - \phi_{(4)}\left(\frac{m_a^2}{\mu_B^2}\right) \left(\frac{\alpha_L}{\pi}\right)^2 \right\}, \quad (5.18)$$

where $\alpha_L = \alpha_L((2/e)\mu_B)$ and $\phi_{(0,2)}(x)$ are given by Eqs. (4.47a), (4.47b), whereas $\phi_{(4)}(x)$ is known in the limit $m_a = 0$,

$$\phi_{(4)}(x=0) = N_F \left[0.92 + \ln \frac{N_F}{2\pi} \alpha_L \right] + 0.71. \quad (5.19)$$

Recall that effective masses $m_a = m_a(M)$ depend on the subtraction point $M = (2/e)\mu_B$ [see Eq. (5.9)]. The definition of the renormalized charge α_L will be assumed to be intact, since the choice of α_L appropriate to the massless case is possible in

Eq. (5.18) even though $m_a \neq 0$.

The threshold functions $\phi_{(0,2)}(x)$ are normalized as $\phi_{(0,2)}(0)=1$. They are determined by the phase space $m^2 + p^2 < \mu^2$ rather than $p < \mu$ and appear as suppression factors. Indeed, one sees from Fig. 32 that $|\phi_{(0,2)}(x)| < 1$, for $x < 1$, i.e., $m_a < \mu_B$. Notice that $\phi_{(2)}(x)$ decreases much faster than $\phi_{(0)}(x)$ as it is given by two- rather than one-particle phase space.

In Eq. (5.18) the function $\phi_{(4)}(x)$ is expected to be suppressed by two- and three-particle phase spaces. Furthermore, at high densities the $\alpha_L^2(\ln\alpha_L)$ terms were found to be negligible for the massless quark gas (see Fig. 30). Therefore, being interested in a rough estimate of mass effects, we restrict ourselves to the Born approximation of Eq. (5.18) and ignore μ_B dependence of quark masses. However, we allow them to vary in a wide range.

$$m_{\phi,\pi} \lesssim 100 \text{ MeV}, \quad m_\lambda \lesssim 400 \text{ MeV}. \quad (5.20)$$

The upper limits are suggested by the MIT bag model³⁸ and nonrelativistic quark models.³⁹

Considering the equation of state with the above input, one finds only 10% variation in the pressure for $\mu_B > 0.5 \text{ GeV}$. The weak dependence on the quark masses is due to the fact that as quarks become heavier the interaction becomes effectively attractive $\phi_{(2)}(x) < 0$, $x > 0.1$.

Thus, quark mass effects do not seem to be significant at relatively high transition densities $> 1 \text{ baryon/fm}^3$.

VI. SUMMARY AND CONCLUSIONS

We have presented the detailed account of results reported in Ref. 1. We have developed systematic perturbation theory for a relativistic fermi gas with non-Abelian gauge interactions. The regularization and subtraction scheme has been formulated in detail at nonzero temperatures. By means of a special reduction technique, the zero-temperature thermodynamic potential of the quark gas has been evaluated up to the second order of the effective fine-structure constant $\alpha_s(M)$ (see Sec. IV D). A tentative phenomenological analysis of the resulting equation of state has been carried out. It has been argued that the neutron-quark-matter phase transition may take place at neutron-matter densities $n_B \lesssim 2 \text{ baryon/fm}^3$ for $\alpha_s(3 \text{ GeV}) \lesssim 0.3$ (see Figs. 30, 31).

An alternative approach for perturbative calculations of the thermodynamic potential Ω has been developed by Freedman and McLerran.¹⁶ They derive an infinite-series expansion for Ω in terms of the various Green's functions^{16a}; the former was subsequently used as a starting point for per-

turbative calculations.^{16b,16c} For comparison, note that our entire discussion was based on the well-known representation for fermion charges given by a single fermion propagator [see Eqs. (2.1), (2.2)]. The final equation of state of a massless quark gas given in Ref. 16c agrees with our results, Eqs. (4.46). However, we have several disagreements with Refs. 16:

(a) A general integral representation of the thermodynamic potential for the *massive* quark gas [cf Eqs. (4.1)] has not been derived in Refs. 16. However, the quark mass is maintained in some expressions. Unfortunately, these results suffer from a lack of definition of the renormalized quark mass m as well as $Z_2(m \neq 0)$ [cf., Eqs. (2.4d), (2.23)]. In particular, these omissions can be consequential in Ref. 16d, where m is considered to be a constant, i.e., independent of the chemical potential μ_B .

(b) In Ref. 16b the regularization of the Fermi surface singularities seem to be *ad hoc*. Calculations are carried out at $1/\beta=0$, however, singularities arising from θ functions have been sidestepped by replacing $\theta(E)$ with the analytic function $\eta(E)$ from Eq. (3.4). Recall that the regularization of these singularities is an essential ingredient of the reduction technique developed in Secs. III, IV.

(c) The appearance of diagrams with two-particle discontinuities such as those in Figs. 18(d), 19(f), 22b, 22c, 22d, etc. has been entirely overlooked. Of course self-energy insertions in Figs. 18(d), 19(f) do vanish in the generalized Landau gauge $\alpha = 1 - (n-2)^2/n$, $n \rightarrow 4$ which was used in Refs. 16b, 16c [see Eq. (A6)]. However, this is not true for discontinuities of vertices in the last diagrams of Figs. 22(b), 22(c), 22(d). Furthermore, it might be very harmful to let $n \rightarrow 4$ at that stage of calculations. The above omission does not affect the final result since the associated diagrams can be shown to cancel between themselves at the zero-temperature limit (cf., Sec. IV).

(d) Equations. (5.12), (5.13) have been employed in Refs. 16c, 16d without making a distinction between two different charges $\alpha_{L,H}$ which are related by Eq. (4.52) (see Fig. 29).

(e) Phenomenological models of Ref. 16d assume that the per baryon energy changes continuously through the phase-transition point in contradistinction to our general conclusion drawn in Sec. V B.

In conclusion, we will briefly discuss possible implications of our results. At present, the ultradense stellar objects⁹ and heavy-ion collisions¹² appear to be the only candidates to which the ideas of a quark gas may be applicable.

The first candidate has been extensively studied in the framework of various neutron-matter models. In particular, equations of state plotted in Fig. 30 predict for the maximum mass neutron stars the following central densities: n_c (baryon/fm³) = 0.5($P - S$)³⁵; 0.9(W),⁴⁰ 1.4($B - J$),⁴¹ 1.7($R - P$).³³ These densities have to be compared with corresponding neutron-quark matter transition densities indicated in Figs. 31, 32. Observe that the former are comparable to the latter. *The comparison suggests that the matter in the central core of superheavy stars exists in the quark rather than in neutron phase provided the color interaction strength $\alpha_s(3 \text{ GeV}) \lesssim 0.3$.*

The remarkable aspect of the above conclusion is that the value of $\alpha_s(3 \text{ GeV}) \lesssim 0.3$ appears to be consistent with the phenomenology of QCD.³²

Turning to heavy-ion collisions we note that relevant densities n_c are those given in the center of mass of two ions

$$n_c = n_0 [2(1 + E_L/M)]^{1/2},$$

where $n_0 \sim 0.16$ baryon/fm³ is a typical nuclear-matter density; M is the mass of colliding nuclei and E_L is the laboratory energy of the incident nucleus. The present operating range of the Beve-lac energies $E_L < 3M$ ensures the neutron-matter densities to be $n_c < 3n_0 \approx 0.5$ baryon/fm³. Hence, the exciting possibility of quark matter production is suggested for relatively weak-interaction strengths $\alpha_s(3 \text{ GeV}) \approx 0.2$.

Clearly, the feasibility of quark matter production requires sufficiently accurate knowledge of $\alpha_s(3 \text{ GeV})$. There are other uncertainties such as those due to the nuclei's finite size effects and the nonstationary character of collisions, which may affect our naive estimates. These questions require a further investigation.

ACKNOWLEDGMENT

I am pleased to acknowledge a kind hospitality extended to me at the Center for Theoretical Physics, MIT. I thank E. Eichten, K. Johnson, A. K. Kerman, F. Low, E. Moniz, J. Negele, and J. Willemsen for many stimulating conversations and the constant encouragement. I am es-

pecially grateful to J. Negele for pointing out to me an error in the equations of state of neutron matter exploited initially. This work was supported in part through funds provided by ERDA under Contract No. EY-76-C-02-3069.*000

APPENDIX

Here we will give general expressions of the renormalization constants $Z_{1,2,3}(M)$ (see Sec. II) in the lowest nontrivial order in the covariant gauge, i.e., for an arbitrary gauge parameter α . Relevant diagrams are given by the quark and gluon self-energies [see Eq. (2.23a), (2.47)] and the quark-gluon vertex [see Eq. (2.32)]. They have been evaluated using Feynman rules of Fig. 1 with $m = \mu = 1/\beta = 0$. Calculations are straightforward, however lengthy. They give

$$Z_1^{(2)} = -\Gamma_{1(\psi)}^{(2)}(-M^2) - \Gamma_{1(G)}^{(2)}(-M^2), \quad (\text{A1})$$

$$Z_2^{(2)} = -\Sigma_1^{(2)}(-M^2), \quad (\text{A2})$$

$$Z_3^{(2)} = \pi_0^{(2)}(-M^2), \quad (\text{A3})$$

with

$$\Gamma_{1(\psi)}^{(2)}(-M^2) = \alpha(n-2)(C_F - \frac{1}{2}C_A)F(n, M), \quad (\text{A4})$$

$$\Gamma_{1(G)}^{(2)}(-M^2) = \frac{3}{2}(1+\alpha)(n-2)\frac{1}{2}C_A F(n, M), \quad (\text{A5})$$

$$\Sigma_1^{(2)}(-M^2) = \alpha(n-2)C_F F(n, M), \quad (\text{A6})$$

$$\pi_0^{(2)} = \left\{ \left[\frac{3n-2}{n-1} + (2n-7)(1-\alpha) - \frac{n-4}{4}(1-\alpha)^2 \right] C_A - 4 \left(\frac{n-2}{n-1} \right) N_F D_F C_F / D_A \right\} F(n, M), \quad (\text{A7})$$

where

$$F(n, M) = -\frac{(M^2)^{n/2-2} \Gamma^2(n/2-1) \Gamma(3-n/2)}{(4\pi)^{n/2} \Gamma(n-2)} \frac{1}{n-4} 4\pi\alpha_s. \quad (\text{A8})$$

In Eq. (A1) contributions from the quark gluon vertex $\Gamma^{(0)}$ and triple gluon vertex $M_2^{(0)}$ have been shown explicitly. Quantities N_F , $D_{F(A)}$, and $C_{F(A)}$ determine the number of flavors, dimension of the quark (gluon) representation, and eigenvalue of the second Casimir operator in the same representation, respectively.

¹V. Baluni, MIT Report No. 591, 1977 (unpublished); Phys. Lett. **72B**, 381 (1978).

²D. Gross and F. Wilczek, Phys. Rev. D **8**, 3633 (1973); **9**, 980 (1974).

³H. Georgi and H. D. Politzer, Phys. Rev. D **9**, 416 (1974).

⁴G. Sterman and S. Weinberg, Phys. Rev. Lett. **39**, 1436 (1977).

⁵T. Kinoshita, J. Math. Phys. **3**, 650 (1962).

⁶T. D. Lee and M. Nauenberg, Phys. Rev. **133**, B1549 (1964).

⁷K. Wilson, Phys. Rev. **179**, 1499 (1969).

⁸N. Itoh, Prog. Theor. Phys. **44**, 29 (1970).

⁹J. C. Collins and M. J. Perry, Phys. Rev. Lett. **34**, 1353 (1975). The importance of the asymptotic freedom for a perturbative analysis of the high-density quark gas was first pointed out by these authors.

- ¹⁰K. Brecher and G. Caporaso, *Nature* **259**, 377 (1976).
- ¹¹G. Baym and S. A. Chin, *Phys. Lett.* **62B**, 241 (1976).
- ¹²G. F. Chapline, Jr. and A. K. Kerman, Livermore report 1977 (unpublished).
- ¹³G. Chapline, Jr. and M. Nauenberg, (a) *Nature* **264**, 235 (1976); (b) *Phys. Rev. D* **16**, 450 (1977).
- ¹⁴B. A. Freedman and L. D. McLerran, MIT report, 1976 (unpublished).
- ¹⁵M. B. Kislinger and P. D. Morley, *Phys. Lett.* **67B**, 371 (1977).
- ¹⁶B. A. Freedman and L. D. McLerran, *Phys. Rev. D* (a) **16**, 1130 (1977); (b) **16**, 1147 (1977); (c) **16**, 1169 (1977); (d) **17**, 1109 (1978).
- ¹⁷(a) L. D. Faddeev, *Teor. Mat. Fiz.* **1**, 3 (1969) [*Theor. Math. Phys.* **1**, 1 (1969)]. (b) L. D. Faddeev and V. Popov, *Phys. Lett.* **25B**, 29 (1967).
- ¹⁸For an alternative derivation based on the method of Ref. 17(b), see C. Bernard, *Phys. Rev. D* **9**, 3312 (1974).
- ¹⁹The integration over the field of anticommuting elements $(\psi_i, \bar{\psi}_i, c_i, c_i^*)$ is discussed by F. A. Berezin, in *Methods of Second Quantization* (Academic, New York, 1966). It is uniquely defined by the rules: $\int d\psi_i = 0$, $\int \psi_i d\psi_i = 1$. Notice that any function $f(\psi_i)$ is reducible to a linear form in ψ_i since $\psi_i^2 = 0$ etc.
- ²⁰The Euclidean four notations are adopted, $x^\mu = (\vec{x}, \tau)$. The metric is $g^{\mu\nu} = -\delta^{\mu\nu}$, $\mu = 1, \dots, 4$. Correspondingly, all Dirac matrices are anti-Hermitian $\gamma^{\mu\dagger} = -\gamma^\mu$. The matrices λ_i and T_i stand for generators G_i of the gauge group in the quark (fundamental) and gluon (regular) representations, respectively. They obey the Lie algebra $[G_i, G_j] = i C_{ijk} G_k$ with structure constants C_{ijk} given by $C_{ijk} = i (T^i)_{jk}$.
- ²¹G. 't Hooft and M. Veltman, *Nucl. Phys.* **B44**, 189 (1972); C. G. Bollini and J. J. Giambiagi, *Phys. Lett.* **40B**, 566 (1972).
- ²²G. 't Hooft, *Nucl. Phys.* **B61**, 455 (1973).
- ²³B. W. Lee and J. Zimm-Justin, *Phys. Rev. D* **5**, 3137 (1972).
- ²⁴A. A. Abrikosov *et al.*, *Methods of Quantum Field Theory in Statistical Physics* (Prentice-Hall, Englewood Cliffs, N.J.).
- ²⁵D. Bohm and D. Pines, *Phys. Rev.* **92**, 609 (1953).
- ²⁶M. Gell-Mann and K. A. Brueckner, *Phys. Rev.* **106**, 364 (1957).
- ²⁷E. S. Fradkin, *Nucl. Phys.* **12**, 465 (1959) and references therein.
- ²⁸I. A. Akhiezer and S. V. Peletminskii, *Zh. Eksp. Teor. Fiz.* **38**, 1829 (1960) [*Sov. Phys. JETP* **11**, 1316 (1960)].
- ²⁹W. E. Caswell and F. Wilczek, *Phys. Lett.* **B49**, 291 (1974).
- ³⁰For a comprehensive review of neutron-matter models, see V. Canuto, *Ann. Rev. Astron. Astrophys.* (a) **12**, 167 (1974); (b) **13**, 335 (1975).
- ³¹W. E. Caswell, *Phys. Rev. Lett.* **33**, 244 (1974); D. R. T. Jones, *Nucl. Phys.* **B75**, 531 (1974).
- ³²M. Ansourian and V. Baluni, report (unpublished) and references therein.
- ³³V. A. Pandharipande, *Nucl. Phys.* **A178**, 123 (1971).
- ³⁴H. A. Bethe and M. B. Johnson, *Nucl. Phys.* **A230**, 1 (1974). The equation of state $B-J$ in Fig. 30 is according to Table 4a in Ref. 30(b).
- ³⁵V. A. Pandharipande and R. A. Smith, *Nucl. Phys.* **A237**, 507 (1975). The equation of state $P-S$ in Fig. 30 predicts a transition to solid neutron phase at $\mu \approx 450$ MeV.
- ³⁶J. D. Walecka, *Ann. Phys. (N.Y.)* **83**, 491 (1974). The equation of state W in Fig. 30 is according to Table 7 in Ref. 30(b).
- ³⁷L. D. Landau and E. M. Lifshitz, *Statistical Physics* (Pergamon, New York, 1958).
- ³⁸T. DeGrand, R. Jaffe, K. Johnson, and J. Kiskis, *Phys. Rev. D* **12**, 2060 (1975).
- ³⁹See, e.g., S. Weinberg, in *A Festschrift for I. I. Rabi*, edited by Lloyd Motz (New York Academy of Sciences, New York, 1977).
- ⁴⁰S. A. Chin and J. D. Walecka, *Phys. Lett.* **52B**, 24 (1974).
- ⁴¹R. C. Malone, M. B. Johnson, and H. B. Bethe, *Astrophys. J.* **199**, 41 (1975).